JACS Au
AN OPEN ACCESS JOURNAL OF THE AMERICAN CHEMICAL SOCIETY

pubs.acs.org/jacsau
Perspective

Alkaline Hydrogen Evolution Reaction Electrocatalysts for Anion Exchange Membrane Water Electrolyzers: Progress and Perspective

Yiming Zhu,[#] Ling Li,[#] Hongfei Cheng, and Jiwei Ma*

Cite This: *JACS Au* 2024, 4, 4639−4654
Read Online

ABSTRACT: For the aim of achieving the carbon-free energy scenario, green hydrogen (H_2) with non-CO_2 emission and high energy density is regarded as a potential alternative to traditional fossil fuels. Over the last decades, significant breakthroughs have been realized on the alkaline hydrogen evolution reaction (HER), which is a fundamental advancement and efficient process to generate high-purity H_2 in the laboratory. Based on this, the development of the practical industry-oriented anion exchange membrane water electrolyzer (AEMWE) is on the rise, showing competitiveness with the incumbent megawatt-scale H_2 production technologies. Still, great challenges lie in exploring the electrocatalysts with remarkable activity and stability for alkaline HER, as well as bridging the gap of performance difference between the three-electrode cell and AEMWE devices. In this perspective, we systematically discuss the in-depth mechanisms for activating alkaline HER electrocatalysts, including electronic modification, defect construction, morphology control, synergistic function, field effect, etc. In addition, the current status of AEMWE is reviewed, and the underlying bottlenecks that impede the application of HER electrocatalysts in AEMWE are summarized. Finally, we share our thoughts regarding the future development directions of electrocatalysts toward both alkaline HER and AEMWE, in the hope of advancing the commercialization of water electrolysis technology for green H_2 production.

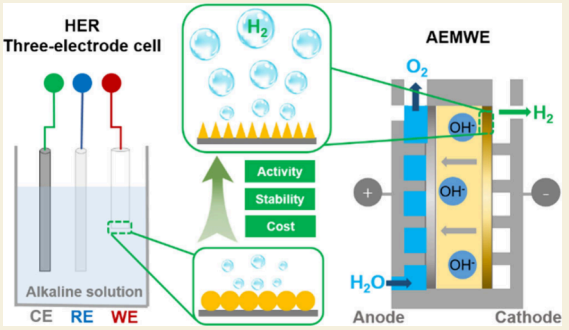

KEYWORDS: *alkaline hydrogen evolution reaction, electrocatalysts, mechanism investigation, anion exchange membrane electrolyzer*

1. INTRODUCTION

The rapidly increased industrial production and human activities are the main contributors to the massive greenhouse gas emissions, leading to global warming and environmental pollution. In order to alleviate this negative effect, most countries have proposed the carbon-free energy scenario, which aims at employing renewable and green energy sources as alternatives to replace the traditional fossil fuels, in an effort to realize zero-carbon emission by 2060.[1−5] Over the past decades, hydrogen (H_2), with a high energy density, light weight, and clean combustion product, has been recognized as an important energy source that could lead to the next generation of energy revolution.[6−9] Currently, the methods for synthesizing H_2 are flexible and diverse, among which methane reforming produces more than 95% of the total H_2. Although it possesses the merits of low cost and high conversion efficiency, the issue of the high carbon emission in this process is also problematic; thus, the generated H_2 is usually called "grey H_2".[10−12] Therefore, water electrolysis, the use of electricity to convert H_2O molecules to hydrogen and oxygen, has attracted more attention because it enables the decarbonized process and produces H_2 with high purity. In addition, this technology is becoming more promising and competitive in terms of cost thanks to the global electricity surplus.[13−15]

Water electrolysis consists of the hydrogen evolution reaction (HER) on the cathodic side and oxygen evolution reaction (OER) on the anodic side, in which HER can be categorized as two reaction avenues based on the employed electrolyte media, specifically, the acidic medium and the alkaline medium.[16−18] As a kind of typical heterogeneous reaction, HER requires the participation of electrocatalysts to facilitate the kinetics and improve performance. The acidic HER is a quite simple reaction process that only involves the adsorption and combination of the hydrogen intermediates; thus, many research achievements regarding electrocatalysts have been realized in this field.[19−24] In contrast, the alkaline HER usually exhibits poor activity and stability due to the sluggish water cleavage step involved. Moreover, compared

Received: September 26, 2024
Revised: November 6, 2024
Accepted: November 13, 2024
Published: November 21, 2024

https://doi.org/10.1021/jacsau.4c00898
JACS Au 2024, 4, 4639−4654

with the acidic water electrolysis, the alkaline electrolyzer with the advantages of mature manufacture technology and low operating cost stands out and dominates the commercial H_2 production market, which urges us to explore the efficient electrocatalysts with satisfied performances toward alkaline HER.[25−27] As is known to all, it is more essential to prepare suitable electrocatalysts through an in-depth understanding of the reaction process than through a lot of trial-and-error attempts, so as to avoid wastage of resources as well as time and to provide guidance for other research areas.[28−30] Therefore, a summary and analysis regarding the facilitation mechanism of previously published papers on alkaline HER electrocatalysts would be extremely meaningful.

At present, there are three mainstream water electrolysis technologies on the market, namely, alkaline water electrolyzer (AWE), proton exchange membrane water electrolyzer (PEMWE), and anion exchange membrane water electrolyzer (AEMWE). In general, these three electrolyzers all require the electrocatalysts to facilitate efficiency and the separators to separate the anode and cathode. Meanwhile, compared with the traditional hydrogen production approaches, they can be operated under a much lower temperature. However, many detailed differences also exist among the AWE, PEMWE, and AEMWE. Specifically, AWE is a well-matured technology, which uses an alkaline solution as the electrolyte. Although the non-noble metals can be accepted as catalysts to reduce the construction cost, their poor activity has also limited the overall operation efficiency of AWE. Moreover, the high ohmic loss and sluggish conductivity derived from the thick diaphragm in AWE result in a low maximum operating current density, slower startup speed, and poor safety under fluctuating conditions. And the generated H_2 from AWE always requires a further purification process. In contrast, the proton exchange membrane with accelerated proton movement ability and thin thickness is usually employed in PEMWE, resulting in the fast dynamic response speed and high operating current density and making it especially suitable for coupling with the intermittent energy sources. The primary restriction that impedes the commercialization of PEMWE is the high cost of catalysts and facilities. Notably, AEMWE is a newly emerging technology that simultaneously has the advantages of AWE and PEMWE. It works in alkaline or pure water conditions, which allows the AEMWE to use the inexpensive non-noble metals as the catalysts, and the capital cost for producing H_2 in AEMWE can be greatly reduced. In addition, the costs of all components in AEMWE, including the porous transport layer and bipolar plate, are lower than those in PEMWE. Moreover, the accepted anion exchange membrane in AEMWE is more conductive and thinner than the diaphragm used in AWE; thus, AEMWE shows a similar large operating current density and quick response rate as PEMWE. Furthermore, AEMWE also has the merits of no leakage, small size, easy to handle, and high stability; thus, it is considered as a competitive technology for large-scale H_2 production.

Exploring the high-performance alkaline HER catalysts is one of the essential preconditions to realize the efficient H_2 production in AEMWE.[31−33] However, unlike the laboratory-scale half cells where the catalytic performance is measured only at the current density of 10 mA cm^{-2}, industry-scale AEMWE needs to be operated for tens of thousands of hours in strong alkaline medium and under large current densities in the range of 200−1000 mA cm^{-2}, which requires the HER electrocatalysts to possess much higher long-term stability.[34−39] Meanwhile, the limited mass transport and poor ionic conductivity derived from the membrane, as well as flowing electrolyte and high currents, make it difficult for electrocatalysts to exhibit the comparable catalytic activity in AEMWE.[40−45] Understanding the differences of the water electrolysis technology between laboratory and industry, thereby designing efficient and stable electrocatalysts with appropriate strategies to narrow the performance gap between them, is an important step toward the commercialization of AEMWE for large-scale use, which is currently fraught with challenges.

In this Perspective, we first systematically introduce the reaction principle of the alkaline HER and its representative theoretical descriptors. Then we will share our understandings and opinions on the activation strategies of the alkaline HER electrocatalysts, including electronic modification, defect construction, morphology control, field effect, and synergistic function, in light of our recent research achievements and other published results. Subsequently, we briefly introduce the component of the AEMWE device, focusing on its cathodic catalyst. A special emphasis will be put on discussing the gaps between the performances of electrocatalysts in laboratory tests and in the industrial implementation, which are essential for promoting the commercial applications of AEMWE. Finally, we will propose the possible future direction in the development of alkaline HER eletrocatalysts toward practical AEMWE. We believe the prospect of the alkaline H_2 production technology is on the rise; therefore, we hope this perspective can provide inspiration and attract more efforts in the research community.

2. HER IN ALKALINE MEDIUM

2.1. Reaction Mechanism of Alkaline HER

HER is a half-cell reaction that takes place at the cathodic side of the water electrolysis, which involves only the transfer of two electrons. The HER mechanisms are obviously different, according to the adopted electrolytes. As we mentioned before, only the adsorption and binding of the H intermediates happen in acidic HER, whereas the reaction processes for alkaline HER are more complicated and are shown below:

$$H_2O + e^- \rightarrow H^* + OH^- \text{ (Volmer step)} \quad (1)$$

$$H^* + H_2O + e^- \rightarrow H_2 + OH^- \text{ (Heyrovsky step)} \quad (2)$$

$$H^* + H^* \rightarrow H_2 \text{ (Tafel step)} \quad (3)$$

Because the cleavage of the H−OH bond in a water molecule needs more energy, the Volmer step is sluggish and limits the supply of protons for the following reaction steps (Heyrovsky and Tafel steps).[7−9] Thus, the overall alkaline HER usually has poor kinetics, exhibiting a much higher overpotential than the acidic HER.

2.2. Representative Descriptors of HER

Previous designs for HER electrocatalysts were obtained by trial-and-error attempts, which were costly and time-consuming. Along with a comprehensive combination of experimental results and theoretical calculations, researchers have found that the activity of alkaline HER is positively correlated or volcanically correlated with a series of descriptors.[46−49] The rational use of these descriptors can explain the origin of the activity and provide guidance for further improvement of the catalytic performance.

https://doi.org/10.1021/jacsau.4c00898
JACS Au 2024, 4, 4639−4654

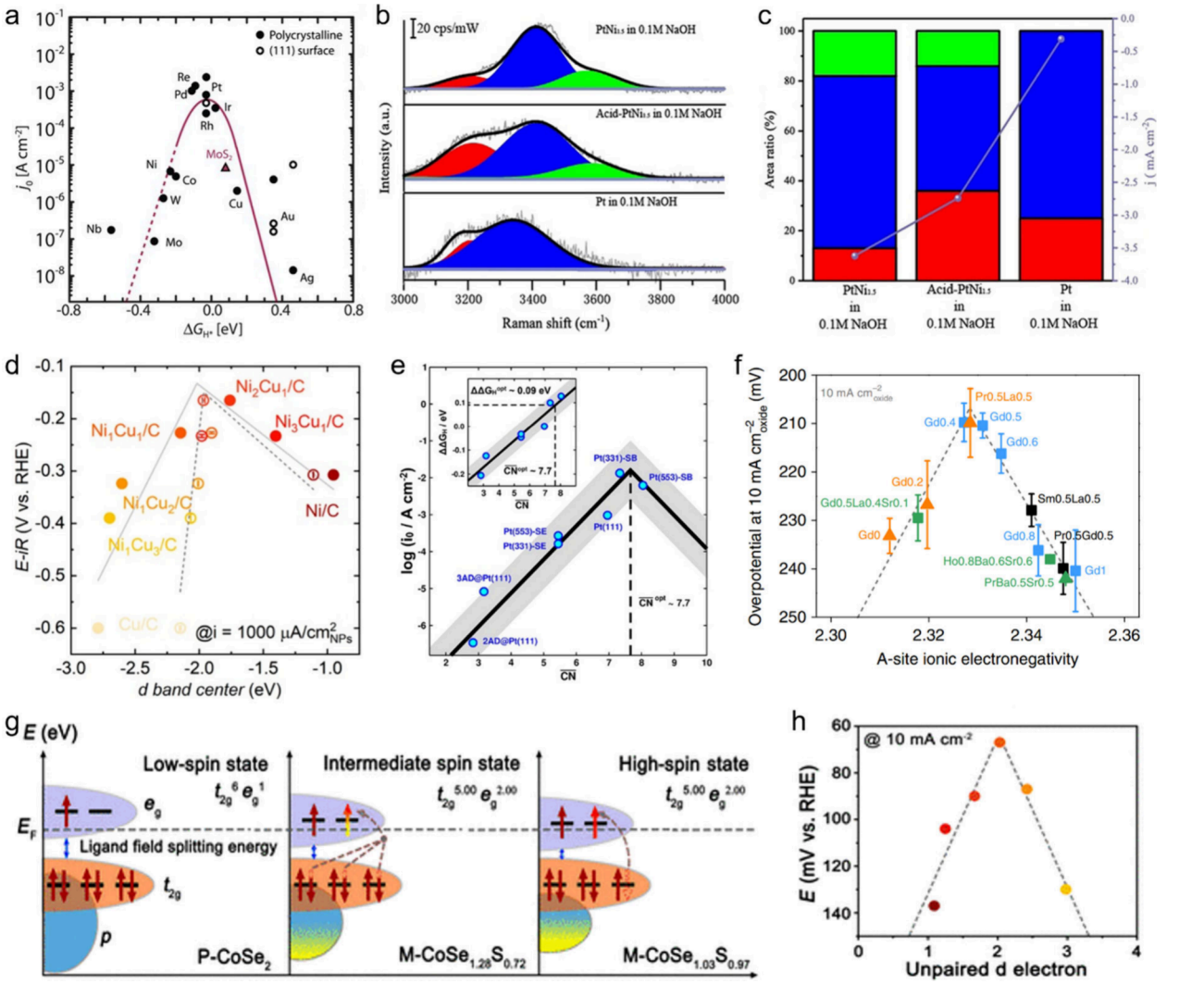

Figure 1. Representative descriptors of HER. (a) The relationship between ΔG_{H^*} and HER current densities on various metals. Reproduced with permission from ref 53. Copyright 2017 AAAS. (b) In situ electrochemical Raman spectra of the O−H stretching mode in 0.1 M NaOH at −0.04 V. These were fitted with three Gaussians (red: tetrahedrally coordinated water; blue: trihedrally coordinated water; green: dangling O−H bonds). (c) The relationship between the area ratio of the three peaks and the overpotentials at −0.04 V. Reproduced with permission from ref 58. Copyright 2020 Wiley-VCH. (d) The d band center vs overpotential on the studied catalysts. Reproduced with permission from ref 64. Copyright 2020 American Chemical Society. (e) Relationship between the coordination numbers and the current densities on Pt materials. Reproduced from ref 69. Available under a CC-BY-NC-ND license. Copyright 2017 The Authors. (f) Correlations between the A-site ionic electronegativity and HER overpotentials on perovskites. Reproduced from ref 72. Available under a CC-BY 4.0 license. Copyright 2019 The Authors. (g) Schematic energy band diagrams of these catalysts. (h) Volcano relationship between the HER activity and the unpaired d-electron number of different catalysts. Reproduced from ref 73. Available under a CC-BY 4.0 license. Copyright 2023.

2.2.1. ΔG_{H^*}, ΔG_{OH^*}, and Interfacial Water. As revealed in the above alkaline HER process, adsorbed H* participates in all reaction steps, and thus an available theory of hydrogen binding energy (HBE) based on Sabatier principles is derived. Specifically, HBE indicates that the HER performance is closely related to the H* binding strength (ΔG_{H^*}).[50−52] As shown in Figure 1a, researchers have plotted the relationship between the experimental HER current densities and the calculated ΔG_{H^*} of various metals, from which a volcano trend can be directly found.[53] It can be seen that when ΔG_{H^*} is less than 0, this means that the binding strength of H* is too strong, which will hinder the release of formed H_2. When ΔG_{H^*} is greater than 0, the binding strength of H* is too weak, which is detrimental to H* adsorption and combination. Apparently, Pt is located at the top of the volcano with ΔG_{H^*} close to zero, indicating that a moderate H* binding strength leads to the best HER performances and the smallest overpotential.[54,55] Recently, Sun's group has also successfully employed the ΔG_{H^*} to predict the excellent alkaline HER activity of Ni_3N/Ni catalysts. They found that the existence of interfacial sites between Ni_3N and Ni can greatly reduce the ΔG_{H^*} and leads to the best catalytic performances.[56] Therefore, the successful applications of ΔG_{H^*} on both noble and non-noble metal catalysts indicate that it is a classic and universal descriptor for anticipating and evaluating the HER performances of electrocatalysts. However, it is noted that this theory also has its own limitations. For example, MoS_2 shows a high overpotential in HER experiment but possesses a suitable ΔG_{H^*} value.[53] This is because ΔG_{H^*} is a thermodynamic descriptor, while there are many other kinetic conditions simultaneously affecting the HER rate.

https://doi.org/10.1021/jacsau.4c00898
JACS Au 2024, 4, 4639−4654

Moreover, the alkaline HER also involves the step of OH^- adsorption, which is also identified as a critical descriptor. Cao's group fixed the contributions from ΔG_{H^*} and ΔG_{H_2O} to solely investigate the relationship between the OH^- kinetics and the HER activity. Based on the experimental and density functional theory (DFT) calculations, they found that the ΔG_{OH^*}, which refers to the interaction strength between OH^- and the catalyst surface, should not be too weak or too strong. When the metal element moves left in the periodic table, the ΔG_{OH^*} will become stronger and the corresponding d-state will rise in energy. Thus, ΔG_{OH^*} is proved as an available descriptor for alkaline HER.[57] On the other hand, Sun and colleagues used in situ Raman spectroscopy to first evidence the direct correlation between the interfacial water structure and HER activity (Figure 1b, c). They observed that the adsorbed water structure in the first layer will convert from proton acceptors to donors with the increasing pH. The activity tendency for interfacial water structure is the tetrahedrally coordinated water > the trihedrally coordinated water > the dangling O−H bonds, indicating that the electrocatalytic performance of an alkaline HER catalyst can be predicted by revealing its interfacial water structure.[58]

2.2.2. Electronic Descriptors. In fact, through modulating the electronic structures of the catalysts, the binding energy of the reaction including intermediates H*, OH*, and H_2O on the catalyst surface, i.e., ΔG_{H^*}, ΔG_{OH^*}, and interfacial water structure, can be directly influenced, thus enabling the modulation of the HER activity. These modulation strategies are often referred to as the electronic descriptors, including d-band center, coordination number, electronegativity, and spin state.

2.2.2.1. d-Band Center. In the field of catalysis, the d-band theory proposed by Hammer and Nørskov in 1995 has been proven to be one of the best theories to describe the catalytic activity of transition metals. The theory suggests that when a reaction occurs, the intermediate tends to form bond with the metal sites, since the electrons in the s orbital of transition metals are usually saturated; thus, only the electrons in the d orbitals are involved in the bonding and determine the strength of the formed bond. Based on this, the d-band center position is actually a descriptor that predicts the catalytic activity of a catalyst by reflecting the adsorption strength of the intermediate. Generally, the upshift of the d-band center results in a stronger adsorption energy of the reaction intermediate. Also, its downward shift will decrease the intermediate adsorption strength.[59−62] Therefore, the binding strength between the metal sites and the H intermediates (M−H) can be revealed from the d-band center position during HER. As discussed in the previous part, too strong or too weak of an adsorption strength will influence the H combination or H_2 release, which in turn is detrimental to the HER catalytic performances. Xu's group has experimentally confirmed a volcano relationship between catalytic activities and the d-band center positions, i.e., a moderate d-band center position is significant for realizing the best HER activity (Figure 1d).[63] Song et al. reported the use of iodine single atoms to manipulate the d-band center of nickel catalysts. As a result, compared with the I−Ni and Ni@C, the I−Ni@C shows the moderate d-band center and thus the best alkaline HER activity.[64] In general, the d-band center is also a typical and universal descriptor that can be applicable to all metal catalysts. However, it should be noticed that the d-band theory is not available in the presence of synergistic adsorption of metal sites with other atoms.[46,47]

2.2.2.2. Coordination Number. For single-atom, cluster, and alloy catalysts, coordination number (CN) demonstrates a profound influence on their catalytic performances.[65−67] Tong and co-workers have carefully regulated the CN of Ru clusters in the range from 2.1 to 2.8 for reactions. They found that the highest activity can be achieved when CN equals 2.8, which is due to the fact that such a high CN results in a strong covalent metal−support interaction and an optimized ΔG_{H^*}.[68] In light of this, CN could serve as an accessible descriptor of HER activity. As shown in Figure 1e, Bandarenka et al. disclosed by combining the theoretical calculations and experimental results together that the platinum (Pt) catalyst shows a volcano-type correlation between its CN and corresponding HER activity, in which a Pt catalyst with a CN value of 7.7 has the best activity.[69] This is because the suitable CN contributes the favorable "concave catalytic centers" on the catalyst, boosting the H adsorption sites and performances. Consequently, CN is a kind of structural descriptor for predicting HER activity. It is also noted that the CN descriptor is usually available to single-atom catalysts and nanoclusters with the exactly defined coordination numbers.[68]

2.2.2.3. Electronegativity. Atomic electronegativity is commonly defined as the ability to attract or donate electrons. Similarly, Liu et al. assumed that the bond electronegativity can be used to describe the electron-holding and electron-donating ability of a chemical bond.[70] They discovered that the intrinsic nature of conducting HER is the electron transfer via the bond between the catalytic structure and the H intermediate. The highest ΔG_{H^*} corresponding to the medium bond electronegativity can be found at the turning point, which is attributed to the evenly distributed electrons in the bond. This is not beneficial for the charge transfer, causing the lowest HER performances.[71] Thus, the bond electronegativity can be introduced as a descriptor for evaluating HER catalysts. In addition, Guan et al. pointed out that the A-site ionic electronegativity (AIE) in the cobalt-based perovskites can be adopted as a descriptor to predict the HER activity.[72] In a typical perovskite structure, the B-sites surrounded by O atoms are proven to be the real active sites for reaction. Different from the previously proposed descriptors that are based on the active B-sites, they employed theoretical calculations to discover a clear volcano correlation between the HER activity and the AIE. The best HER performance with a moderate AIE value is successfully correlated with the optimal electronic states of active B-sites in perovskites to fulfill the Sabatier's principle via the inductive effects and electron exchange interactions between A-sites and B-sites from molecular orbital theory (Figure 1f). The descriptor of electronegativity opens a universal avenue for predicative evaluating the HER performances on binary and even ternary transition metal oxides.[72]

2.2.2.4. Spin States. It is well-known that the spin states of catalysts deeply influence their catalytic behaviors. It has been proven that the interaction between the d-orbital electrons and the reaction intermediates can be adjusted by modifying the spin states of the catalysts, but more attention is being devoted to the field for the aim of discovering the relationship between the catalytic activity and the spin states. In this regard, Gao et al. reported that the spin states of Co atoms can be regulated by partially replacing the Se with S atoms in $CoSe_2$, in which the low-spin (LS) state Co transforms to high-spin (HS) state Co after S introduction.[73] Specifically, as shown in Figure 1g,

https://doi.org/10.1021/jacsau.4c00898
JACS Au 2024, 4, 4639−4654

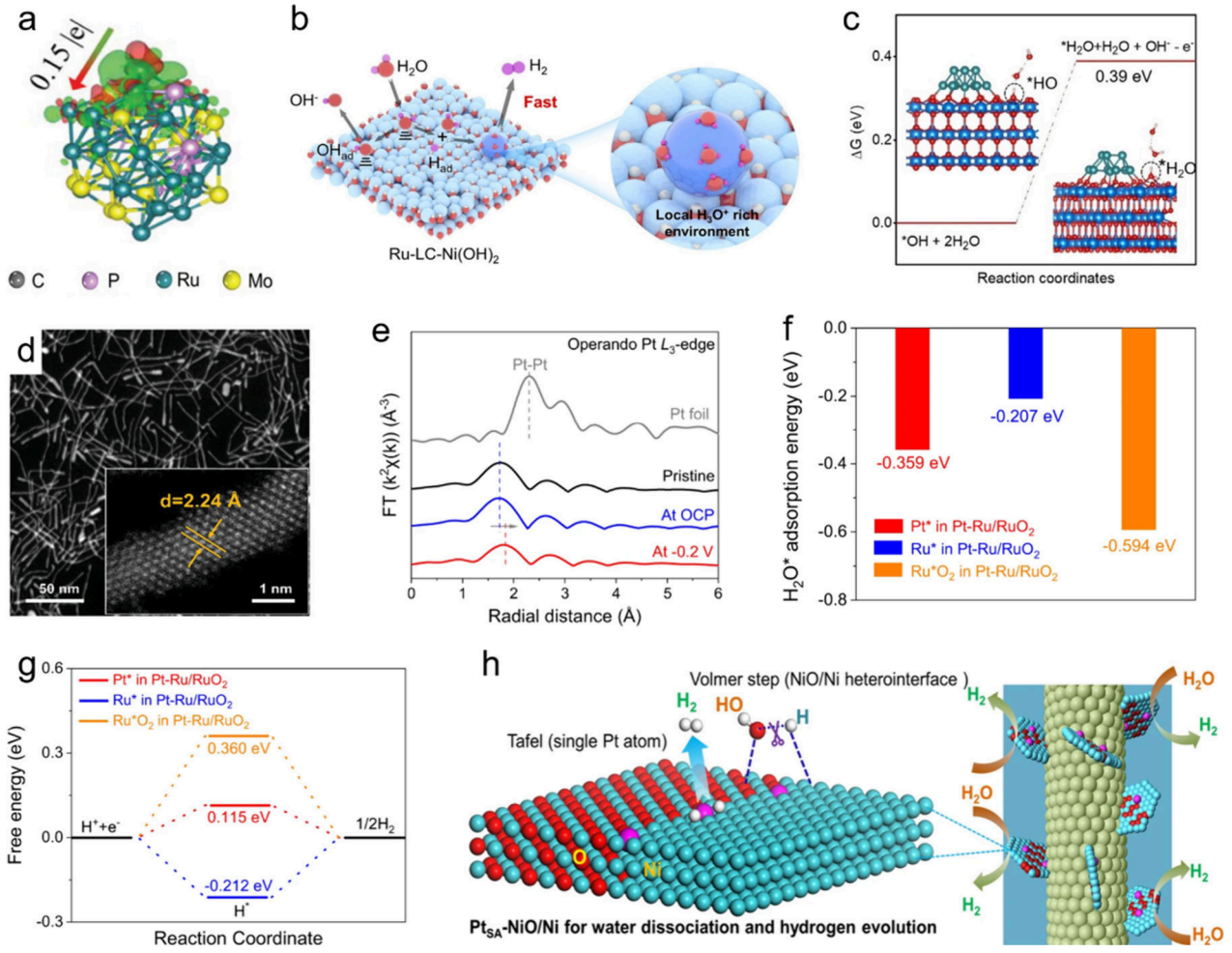

Figure 2. Activation strategies for HER electrocatalysts. (a) Differential charge density distributions for selected single Ru atom in P,Mo−Ru cluster with a value of 0.002 e Å^{-3}. Reproduced with permission from ref 77. Copyright 2022 Wiley-VCH. (b) Schematic diagram of microenvironmental changes on Ru−Ni(OH)$_2$ with low crystallinity. Reproduced with permission from ref 81. Copyright 2024 Wiley-VCH. (c) ΔG value and scheme of alkaline HER on Ru/ac-CeO$_{2-\delta}$. Reproduced with permission from ref 85. Copyright 2024 Wiley-VCH. (d) HAADF-STEM image of the ultrathin SA In−Pt NWs. Reproduced with permission from ref 90. Copyright 2020 Wiley-VCH. (e) The operando Pt L_3-edge EXAFS spectroscopy on Pt−Ru/RuO$_2$ during alkaline HER. The (f) H$_2$O* adsorption energy and (g) H* adsorption free energy values for Pt, Ru and RuO$_2$ sites in Pt−Ru/RuO$_2$. Reproduced from ref 97. Available under a CC-BY 4.0 license. Copyright 2024 The Authors. (h) The mechanism of the Pt$_{SA}$-NiO/Ni network as an efficient catalyst toward large-scale water electrolysis in alkaline media. Reproduced from ref 100. Available under a CC-BY 4.0 license. Copyright 2021 The Authors.

the unpaired electron number in P-CoSe$_2$ is calculated to be 1.03, matching the LS state ($t_{2g}^6e_g^1$), while the unpaired electron numbers rise to 2.03 and 2.98 after incorporating S atoms, indicating the conversion from LS to HS ($t_{2g}^5e_g^2$) states. As a result, they found that the HER activity exhibits a volcanic relationship with the unpaired d-electron, in which M-CoSe$_{1.28}$S$_{0.72}$ with a medium unpaired electron number of 2.03 has the best activity (Figure 1h). Too few or too many unpaired d-electrons will cause too weak or too strong binding strength with the reaction adsorbates, which is averse to promoting HER. Therefore, spin state can also be considered as an electronic descriptor for screening the promising HER electrocatalysts.

Overall, in recent studies, the binding energy is the most classic and available descriptor, especially in predicting the HER activity of the metallic catalysts. However, it should be mentioned that the theoretical models of these descriptors are in fact too simple, whereas the real HER condition is complex and includes issues such as solvation, cationic (K^+, Na^+) influences, etc., which have an impact on the catalyst activity. In addition, for the recently emerging novel catalysts such as diatomic catalysts, metal carbides, and even metal−organic frameworks (MOFs), there is still a necessary requirement to discover a more general descriptor for predicting HER activity. Currently, it is promising to establish a database combining theoretical parameters and experimental results to provide a platform for the systematic and comprehensive exploration of electrocatalysts, through which the structure−property relationships can be predicted quickly and realistically by high-throughput computation, screening, and other related methods. The machine learning method has successfully exhibited the ability to screen the high-performance HER catalyst via the d-band theory. In this regard, we believe that the machine learning method based on simulation and analysis of big data could be a promising and efficient means to establish a universal descriptor in the future, which deserves more attentions.[74,75]

https://doi.org/10.1021/jacsau.4c00898
JACS Au 2024, 4, 4639−4654

3. ACTIVATION STRATEGIES OF ALKALINE HER ELECTROCATALYSTS

To date, the reported HER electrocatalysts with high performance in the alkaline medium are much fewer than those in the acidic medium. Since the reaction mechanism of the alkaline HER is relatively complex, researchers have explored different strategies to boost the catalytic performance of the catalyst from various aspects.[40,42] In this section, we will summarize the activation mechanisms of the reported alkaline HER catalysts and present our own understanding in light of our recent research findings.

3.1. Electronic Structure Modification

Engineering the electronic structure of a catalyst is the most direct and operative strategy to facilitate the alkaline HER rate by improving the conductivity or optimizing the H* adsorption strength. Doping foreign atoms into the host supports to realize the electronic structure modification is commonly reported.[76] For example, Cho et al. designed the P,Mo dual doped Ru ultrasmall nanoparticles embedded in P-doped porous carbon (P,Mo−Ru@PC) for alkaline HER.[77] In comparison with the pristine Ru@PC, the overpotential is decreased from 38 to 21 mV after the incorporation of Mo and P atoms. Detailed investigations revealed by Barder charge analysis indicates that the electron will transfer from Ru to doped Mo and P, causing the stronger H_2O adsorption energy than undoped materials. As we discussed before, the H_2O adsorption energy is an essential HER descriptor, and the stronger the H_2O adsorption, the lower the H_2O dissociation barrier, consequently beneficial for alkaline HER (Figure 2a). Besides metal atoms, the introduction of some nonmetal atoms has likewise been shown to be significant in regulating the electronic structures of the HER catalysts. Su's group adopted the N and Mn dopants to regulate the electronic states of MoS_2. Specifically, the band gap is reduced and the H* adsorption free energy is optimized on N, Mn codoped MoS_2, leading to the excellent alkaline HER performances.[78,79] Given that, doping is certainly a future-proof method for electronic structure modification. However, the variety of doped element species is limited, and not every one of them has a positive effect, so we believe that using theoretical calculations to predict in advance, followed by experimental confirmation, is an important step to avoid trial-and-error attempts.

In addition to the doping method, the electronic structure of active site atoms has also been proven to be effectively modulated by changing the crystallinity of the support.[80] Peng and co-workers revealed that the $Ni(OH)_2$ carrier with low crystallinity can transfer more electrons to Ru single atoms than can the one with high crystallinity, causing the electron-rich Ru sites and constructing a local acidic microenvironment to enhance the alkaline HER (Figure 2b).[81] Furthermore, other strategies including coordination environment tuning are also reported for the optimization of electronic structures toward alkaline HER.[82]

3.2. Defect Construction

Constructing defects in catalysts has always been a hot topic in the field of electrocatalysis, and of course alkaline HER is no exception.[83,84] The incorporation of suitable defects helps to create more unsaturated sites to serve as the active centers for accelerating the catalytic performances. Generally, defects are classified as the anion vacancy and the cation vacancy. First, the anion vacancies, involving the oxygen vacancy, selenium vacancy, and sulfur vacancy, are reportedly beneficial for alkaline HER. Cho et al. synthesized the Ru cluster anchored on oxygen vacancy enriched amorphous/crystalline CeO_2 (Ru/ac-$CeO_{2-\delta}$) for superior alkaline HER.[85] The corresponding activation mechanism is attributed to the oxygen vacancy acting as the Lewis acid sites to enhance the H_2O adsorption energy and cleave the H−OH bond as well as optimize the H intermediates' adsorption energy (Figure 2c). Moreover, Li et al. revealed that introducing the phosphorus vacancy in the MoP can create more electrochemically active sites and facilitate the charge transfer capability to boost the alkaline HER activity.[86]

On the other hand, cation vacancy, specifically metal vacancy, has also been introduced for unlocking the power of electrocatalysts. For instance, Zhang reported the FeOOH with Fe vacancies toward superior alkaline HER. Theoretical results show that, in contrast to anion vacancy, the second neighboring Fe atom near the Fe vacancy is the real HER active site, and the other function of Fe vacancy is optimizing the electronic structure of FeOOH.[87] It is noted that the cation vacancy is more difficult to fabricate compared with the anion vacancy due to the high formation energy. In addition, the introduction of defects is a "double-edged sword", and the catalysts with defects tend to have a poor stability due to the incomplete lattice atoms as well as the recovery and diffusion of the defects during reaction.

3.3. Morphology Control

As an interfacial reaction, the intrinsic activity of alkaline HER is closely related to the number of surface active sites on catalysts. Reasonable control of catalyst morphology is able to expose more surface atoms, maximize the atomic utilization efficiency, and increase the contact area with the electrolyte to improve the catalytic activity.[88] The current commercial HER catalysts are still dominated by Pt nanoparticles (NPs) with a 0D nanostructure, exhibiting a relatively small electrochemical surface area (ECSA). Fabricating 1D nanowires (NWs), 2D nanosheets, and 3D nanoframes with enlarged specific surface areas can effectively resolve the above issue. Also, it has been proven that a large exposed area is also beneficial for the release of generated H_2.[89] In our previous work, we have experimentally demonstrated that the ECSA of the synthesized ultrathin single-atom indium-doped Pt NWs (SA In−Pt NWs) reaches 65.9 $m^2\ g^{-1}$, which is obviously larger than that of the SA In−Pt NPs (58.0 $m^2\ g^{-1}$) (Figure 2d).[90] As a result, SA In−Pt NWs exhibit higher mass and specific activities. Liu and co-workers synthesized the WS_2/WO_3 nanosheets and studied the alkaline HER mechanism. They found that the ultrathin 2D nanosheet morphology of WS_2/WO_3 is beneficial for enhancing the surface area, exposing more active sites and speeding up the charge transfer rate.[91] Although fruitful achievements of morphology engineering have been achieved, by summarizing the literature, we found that cumbersome preparation processes are often required to obtain the special shapes. For example, it is necessary to add protectants and shape-controlling reactants in the reaction solvent, and these organic ligands will adsorb on the surface of the nanomaterials and are difficult to remove. Moreover, the framework structure usually needs an additional etching step, which involves the use of hazardous acid and base reagents.[92] This strategy is currently getting much less attention, and related research reports are gradually decreasing.

https://doi.org/10.1021/jacsau.4c00898
JACS Au 2024, 4, 4639−4654

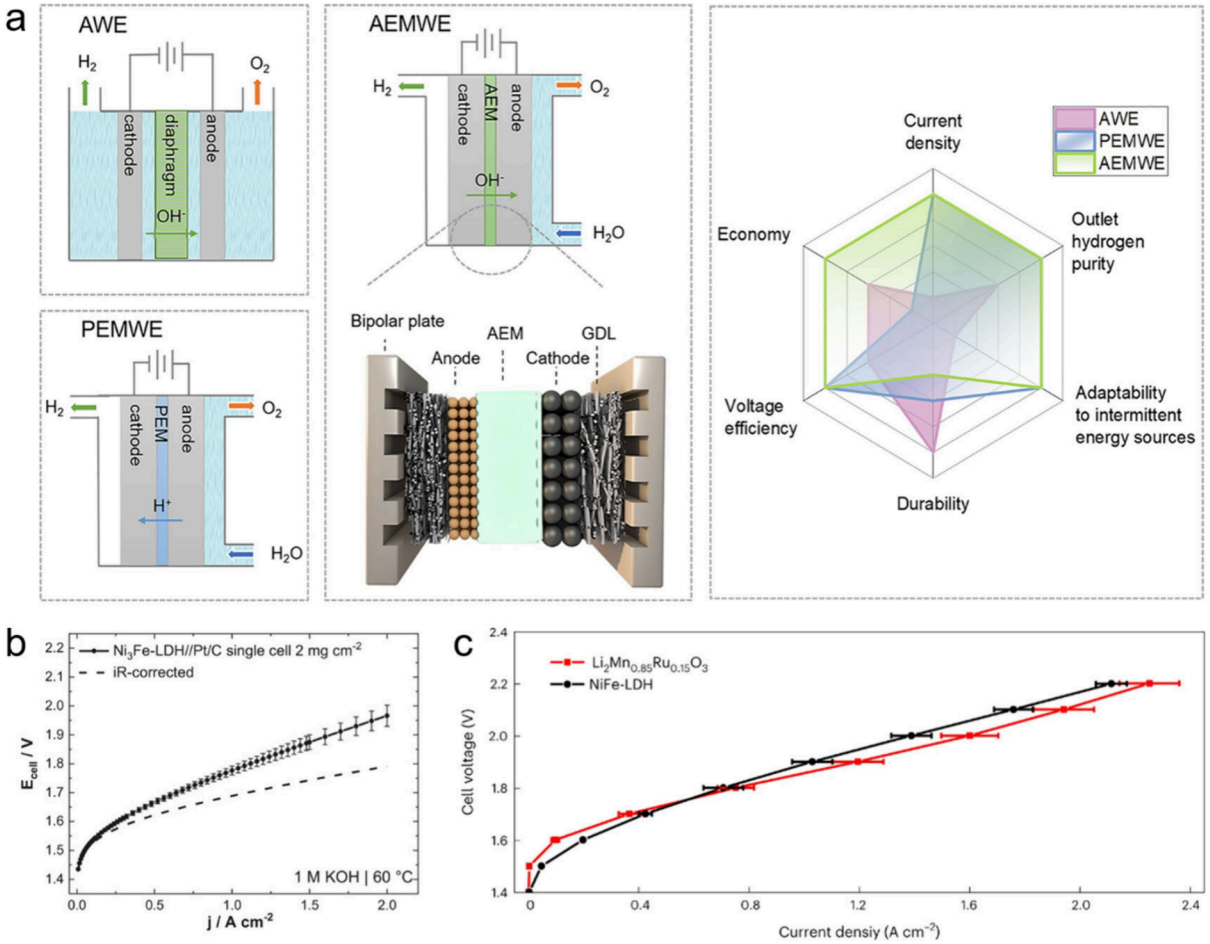

Figure 3. Components of AEMWE. (a) Schematic illustration of AWE, PEMWE, and AEMWE, and their performance comparison. Reproduced with permission from ref 103. Copyright 2024 Elsevier. (b) The AEMWE performances of Ni_3Fe-LDH//Pt/C in 1 M KOH. Reproduced with permission from ref 104. Copyright 2024 Wiley-VCH. (c) The polarization curves of the electrolyzer using $Li_2Mn_{0.85}Ru_{0.15}O_3$ or NiFe-LDH as the anode and Pt/C as the cathode. Reproduced with permission from ref 105. Copyright 2024 Springer Nature.

3.4. Field Effect

Besides changing the physicochemical properties of the catalyst itself, activating the HER catalysts through the implementation of external fields, including the electric field and magnetic field, is also a feasible methodology. For example, after applying an electric field of 5 V on MoS_2, it shows the lowest alkaline HER overpotential of 38 mV at 100 mA cm^{-2}, and its Tafel slope value has fallen to half of that of no electric field.[93] The outstanding activity is attributed to the tuned charge injection and the increased electrical conductivity caused by the additional electric field. In addition, Du et al. found that a lower HER overpotential and Tafel slope are achieved on $NiCo_2S_4$ in 1 M KOH under a moderate magnetic field of 100 mT than the one without magnetic field.[94] Detailed investigations indicate that the added magnetic field has a magnetohydrodynamic (MHD) effect, that is, the Lorentz force caused agitating ions to act as microstirrers to enhance the convection of reactants and products, reducing the polarization resistance and improving the mass transportation. The greatest merit of the external field effect is that it is not detrimental to structure, which can enhance the catalyst activity while maintaining its intrinsic properties. However, this method requires additional energy input and sophisticated instrumentation to precisely modulate the field; thus, its development is still at an early stage, and there is a large room toward industrial application.[95]

3.5. Synergistic Function

The synergistic function is the hotspot of current research on alkaline HER electrocatalysts and is what we particularly wish to highlight in this part.[96] As previously mentioned, the complex alkaline HER usually consists of the water dissociation step and the hydrogen combination step, but the same active sites are commonly monofunctional. Thus, an ideal electrocatalyst should possess an efficient synergistic function, that is, involving separated active sites to activate different reaction steps, respectively. In our latest research results, we have successfully reported a catalyst based on Pt single atoms doped into the heterointerfaced Ru/RuO_2 support ($Pt-Ru/RuO_2$), featuring a low HER overpotential and distinctly enhanced price activity compared with the commercial Pt/C and Ru/C in 1 M KOH solution.[97] Advanced operando EXAFS discovers that at the HER potential of −0.2 V, the main Pt−O bond obviously shifts to a more positive position; this is a signal that the local structure relaxation of Pt caused by the absorbed H*, indicating that Pt single atoms can efficiently promote the H* atom adsorption (Figure 2e). DFT calculations of H_2O adsorption energy further reveal that the RuO_2 sites have the strongest H_2O adsorption ability among all active sites, demonstrating that RuO_2 is the reaction site for accelerating

https://doi.org/10.1021/jacsau.4c00898
JACS Au 2024, 4, 4639−4654

the sluggish H_2O dissociation step (Figure 2f); while in Figure 2g, a Pt single atom has the most optimized H* adsorption free energy, which is consistent with the EXAFS results and further confirms that the function of Pt single atoms is to facilitate the H* combination step. Also, Ru sites show a stronger capability of producing H_2 than do RuO_2 sites. The above characterizations jointly prove that the multiple active sites in Pt−Ru/RuO_2 synergistically increase the alkaline HER performances. Similarly, Lee et al. also reported the use of Pt single atoms on defective CeO_x (Pt_1/CeO_x) as a dual-site HER catalyst with high activity.[98] In this context, CeO_x is active for water adsorption and dissociation, whereas H_2 is formed on Pt single atoms. Also Li's group presented the Ni_3Sn_2−$NiSnO_x$ nanocomposites as the alkaline HER catalyst, in which Ni_3Sn_2 possessed an ideal hydrogen adsorption ability and $NiSnO_x$ facilitated the water dissociation.[99] Yan et al. developed a single-atom Pt immobilized NiO/Ni heterostructure (Pt_{SA}-NiO/Ni) for alkaline HER. It is found that the NiO/Ni heterostructure adjusts OH* and H* adsorption affinity to reduce the water dissociation energy barrier. Simultaneously, the Pt SAs facilitate the H* combination and enhance the HER activity (Figure 2h).[100] All these examples indicate that taking advantage of synergistic function in catalysts can purposely address the problems of sluggish kinetics in alkaline HER. It is also found that the synergistic function is usually induced in the noble metal single-atom catalyst systems. The aim is to largely reduce the amount of precious metals while utilizing the respective functions of single atoms and supports, thereby lowering cost and improving performance.[101] The similar electrocatalyst design concept has also been extended to other electrocatalytic processes with multistep reactions such as carbon dioxide reduction reaction and nitrogen reduction reaction. It is worth noting that the synergistic function exists only in binary or even multimetallic catalysts due to the requirement of multiple active sites, which poses a challenge for the reasonable selection of metal elements in the catalysts, and the controlled fabrications of the catalysts. In addition, the in-depth elucidation of the synergistic function in multisite catalysts and the detailed analysis of the relationship between the structure and catalytic performance particularly require the assistance of various sophisticated techniques for validation, including advanced spectroscopic and microscopic technologies and theoretical calculations, etc., which is a complex and time-consuming task.[102] In any case, we believe that this strategy of precisely designing catalysts will have a promising future in breaking the bottleneck of performance in practical applications of energy conversion.

4. AEMWE

Undoubtedly, the next logical step following the exploration of the efficient alkaline HER electrocatalysts is to employ them in the practical AEMWE.[37−40] In this part, the current status of AEMWE is reviewed, and the underlying bottlenecks that impede the application of HER electrocatalysts in AEMWE are summarized and analyzed.

4.1. The Components of AEMWE

As shown in Figure 3a, the major components of the AEMWE are anion exchange membrane (AEM), gas diffusion layers (GDL), current collectors, clamps, and electrocatalysts. The special AEM is fabricated with the polymer backbones and anion exchange functional groups, which only allows the transfer of anions.[103] GDL has a deep influence on gas bubble management and mass transfer efficiency. Because of the good thermodynamic stability and the capability to passivize under the oxidative potentials, Ni foam or Ni felt is commonly selected as the GDL at the anode side of AEMWE. Meanwhile, in order to prevent carbon corrosion in the oxidative and alkaline environment, porous carbon materials are limited to being used as the GDL at the cathode side. In addition, with excellent corrosion resistance, low start-up resistance, good mechanical strength, and light weight, Ti is currently the best candidate of current collector for PEMWE. However, due to the high costs of raw materials and manufacturing, Ti is relatively expensive. Notably, due to the excellent operation stability in alkaline electrolytes, Ni-plated stainless steel is usually adopted as the current collector. Most importantly, this cheap material can reduce the overall manufacturing cost of AEMWE devices. Generally, the reaction principle of AEMWE is that the circulated H_2O is reduced to H_2 and OH^- at the cathodic side, and the OH^- will simultaneously transfer through the AEM to the anodic side to form the O_2. The operating temperatures and typical discharge H_2 pressure of AEMWE are 50−70 °C and 30 bar, respectively, which are not so harsh conditions as in AWE and PEMWE. It is noted that both sides in AEMWE require the electrocatalysts to overcome the barrier and boost the reaction. To date, the cheap NiFe layered double hydroxides (LDH) and other low platinum group metal (PGM) catalysts with high activity and stability are gradually adopted as the anodic catalyst to replace the commercial RuO_2/IrO_2 in AEMWE (Figure 3b).[104] Our group has successfully discovered the low-amount Ru doped Li_2MnO_3 electrocatalyst ($Li_2Mn_{0.85}Ru_{0.15}O_3$) as the anodic catalyst. By employing the Pt/C in the cathode to fabricate the whole AEMWE cell, $Li_2Mn_{0.85}Ru_{0.15}O_3$ exhibited a high current density of 1.2 A cm^{-2} at 1.9 V, surpassing NiFe-LDH, commercial IrO_2, and many other reported materials (Figure 3c).[105] In this regard, it is found that the 3d transition-metal-based materials are promising candidates for catalyzing the anode side of AEMWE. Nevertheless, the widely used cathodic catalysts in AEMWE are still the Pt black and Pt/C, which are very expensive and show unsatisfactory performances in the alkaline media compared to the acidic media due to the sluggish water dissociation step.[47] Therefore, in our opinion, one restriction that limits the commercialization of the AEMWE lies in the lack of low-cost and high-performance cathodic catalysts, especially the low-noble-metal and non-noble-metal catalysts.

4.2. The Bottlenecks of HER Electrocatalysts in AEMWE

Obviously, a considerable number of published articles have designed high-performance alkaline HER electrocatalysts by various activation strategies in the laboratory; however, only a small number of them have further applied the catalysts in industry-oriented AEMWE. There is a clear gap that prevents the application of laboratory-prepared HER catalysts in practical H_2 production devices. For example, the test temperature and the applied oxidative potential in AEMWE are higher than those in the three-electrode system in the laboratory. The harsher operating environment presents a bigger challenge for the performance of the HER electrocatalyst in AEMWE. Also, vigorous bubbling under the high current densities usually results in a severe catalyst stripping problem, affecting the AEMWE performance. Therefore, we will analyze and summarize three major bottlenecks including

https://doi.org/10.1021/jacsau.4c00898
JACS Au 2024, 4, 4639−4654

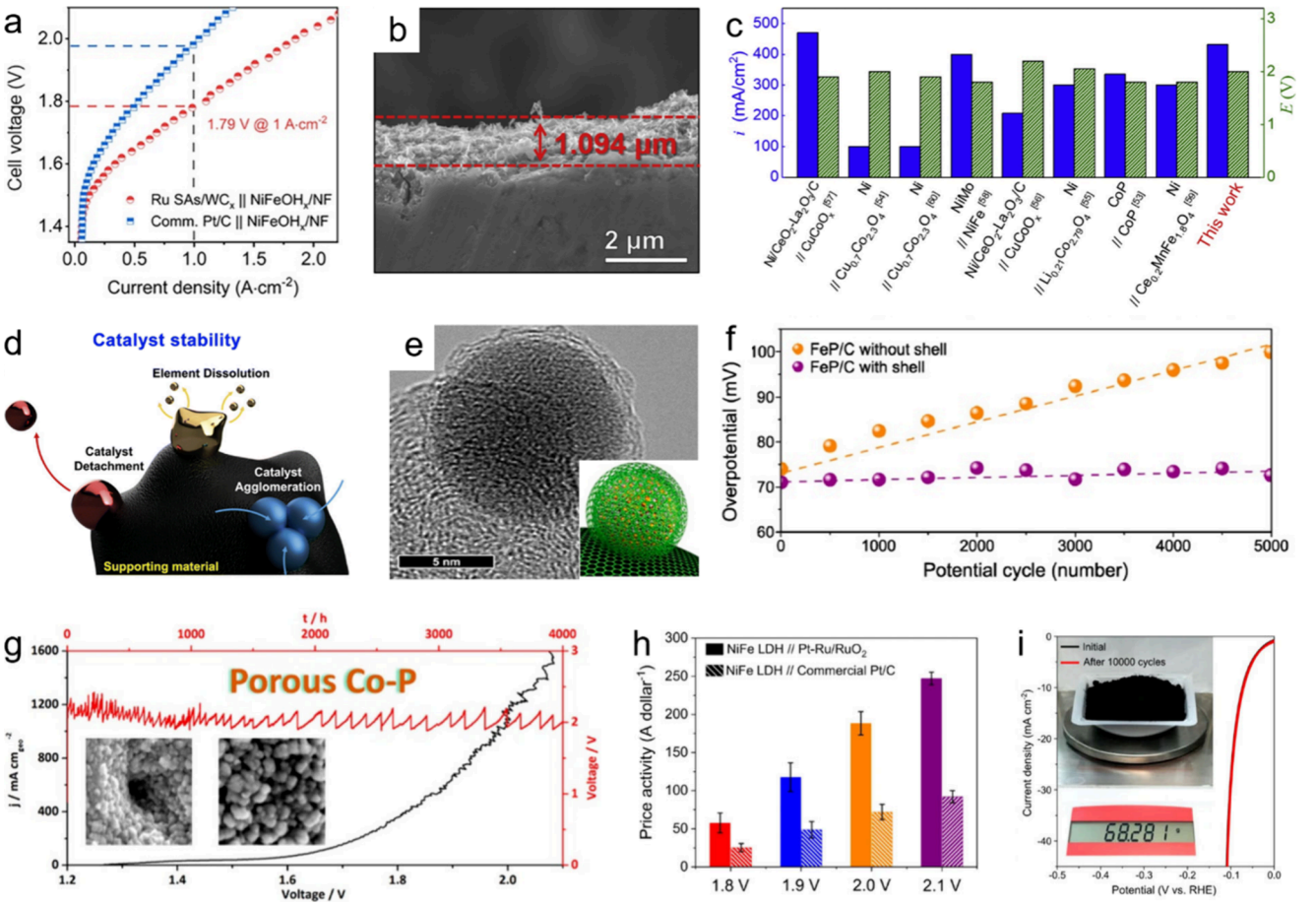

Figure 4. HER electrocatalysts in AEMWE. (a) Polarization curve of Ru SAs/WC_x//$NiFeOH_x$-NF and Pt/C//$NiFeOH_x$-NF in the AEMWE operated at 80 °C. Reproduced with permission from ref 106. Copyright 2024 American Chemical Society. (b) Cross-sectional FE-SEM image of Co_3S_4 NS/NF. (c) Comparison of the reported single cell AEMWE performance using nonprecious metal catalyst. Reproduced with permission from ref 108. Copyright 2020 Elsevier. (d) The challenges of catalyst stability for high-current-density water electrolysis. Reproduced with permission from ref 109. Copyright 2023 Royal Society of Chemistry. (e) TEM image of the carbon-shell-coated FeP nanoparticles. (f) Plots of overpotential vs potential cycle for the data in panel. Reproduced with permission from ref 111. Copyright 2017 American Chemical Society. (g) Chronopotentiometric curves of the porous Co−P//porous Co−P electrolyzer recorded at a constant current density of 1000 mA cm^{-2} with *iR*-correction. Reproduced with permission from ref 112. Copyright 2020 American Chemical Society. (h) Price activities of NiFe LDH//Pt−Ru/RuO_2 and NiFe LDH//commercial Pt/C at various cell potentials (without *iR* correction). Reproduced from ref 97. Available under a CC-BY 4.0 license. Copyright 2024 The Authors. (i) Polarization curves for 10000 cycle tests of FeP with the carbon shell obtained by large-scale synthesis. The inset shows a picture of the product and its weight. Reproduced with permission from ref 111. Copyright 2017 American Chemical Society.

activity, stability and cost, followed with the viewpoints on how to break these barriers based on our own test experiences as well as the reported literature.

4.2.1. Activity. Actually, activity is the most intuitive factor that determines the usage of HER electrocatalysts in AEMWE. Owing to the excellent performance, noble metal catalysts including Pt and Ru still possess the priority. However, the usage and specific loading amount of the noble metal in the catalysts should be minimized in the AEMWE due to the economic concern, which inevitably limits the performance. In addition, the AEMWE is operated under much harsher conditions including higher current density, higher temperature, and stronger corrosion compared with the three-electrode system in the laboratory; thus, many advanced HER catalysts prepared by morphology control and defect engineering easily undergo shape breakage and defect recovery in this process, causing the loss of active sites and activity degradation. So we think that constructing HER catalysts through the synergistic function to activate the AEMWE is more feasible. As depicted in Figure 4a, Wu's group anchored the Ru single atoms onto tungsten carbides (Ru SAs/WC_x) to induce the puncture effect to alleviate the OH blockades and the synergistic effect to accelerate the water dissociation. As a result, only 21 mV is required for Ru SAs/WC_x to reach 10 mA cm^{-2} in alkaline HER.[106] Importantly, such a catalyst-based AEMWE can also exhibit an ultralow potential of 1.79 V at 1 A cm^{-2}, which is superior to the Pt/C counterpart. Moreover, Li et al. designed the Ni single atoms modified ultrasmall Ru nanoparticles (UP-$RuNi_{SAs}$/C) with efficient interaction between Ni SAs and Ru supports.[107] This material delivers a smaller alkaline HER overpotential of 9 mV at 10 mA cm^{-2} and a lower AEMWE cell voltage of 1.95 V at 1 A cm^{-2} compared to those of Pt/C.

In addition, the development of 3d transition-metal-based HER electrocatalysts under alkaline conditions is under active exploration. The research on alkaline HER electrocatalysts mainly focuses on non-noble metal elements such as Ni, Co, Fe, etc. The most essential one is Ni, which shows HER activity and stability higher than those of Co and Fe in the alkaline electrolyte. Notably, the pure Ni cannot satisfy the

https://doi.org/10.1021/jacsau.4c00898
JACS Au 2024, 4, 4639−4654

performance requirement of the practical AEMWE. Thus, it is common to use the alloy and heteroatom doping strategies on Ni to form the Ni-based electrocatalysts including NiMo alloy, NiCo alloy, NiS, Ni_2P, and so on, which can activate the alkaline HER. For example, Wang et al. constructed the cheap NiAlMo catalyst as the cathode in AEMWE. As a result, it only requires 2.086 V to reach the current densities of 2 A cm^{-2}, which is comparable to the performance of the noble metal Pt. Considering the extremely low cost, more attention should be further devoted on enhancing the AEMWE activity of Ni-based electrocatalysts in the future.

Moreover, the components of AEMWE involve the membrane and flowing electrolytes, which are far more complex than the three-electrode system in the laboratory. Thereby unavoidable influences including the sluggish transport issues arise, limiting the activity of HER electrocatalysts in AEMWE. Also, gas bubbles are violently generated under high currents, which will block the active sites and destroy the catalyst−electrolyte interface. To eliminate these negative effects, directly depositing the metals on Ni foam or carbon paper with good conductivity and porous structure to construct the whole supported catalysts may be available.[39] As depicted in Figure 4b, the Co_3S_4 nanosheets on Ni foam (Co_3S_4 NS/NF) were prepared by Choi and co-workers via the electrodeposition method. Using the Co_3S_4 NS/NF as the cathodic catalysts, the assembled AEMWE exhibited a current density of 431 mA cm^{-2} at 2.0 V. Although the AEMWE performance of Co_3S_4 NS/NF is hardly comparable to that of Pt/C, it has surpassed most of the reported non-noble metal catalysts (Figure 4c).[108] The promotion is possibly attributed to the enhanced conductivity and rapid gas release caused by the NF support.

Furthermore, unlike the three-electrode system testing in the laboratory, the parameters of AEMWE testing are numerous. We hereby call for the establishment of standardized operating and reporting protocols including catalyst loading amount, test temperature, electrolyte concentration, and measured voltage to properly evaluate the activity of HER catalysts in AEMWE.

4.2.2. Stability. The steady operation for a long period is the prerequisite for the widespread application and commercialization of AEMWE. However, the stability of most HER electrocatalysts can last for only several hours in the practical water electrolyzer, which is far from meeting the rigorous requirement of AEMWE (80,000 h). Looking deeper, the limited factors that undermine the stable operation of HER electrocatalysts can be categorized as chemical degradation and mechanical degradation. As shown in Figure 4d, the chemical degradation mainly refers to the phenomenon that under the harsh operating conditions of AEMWE (high currents and strong alkalinity), the catalyst will experience severe reconstruction, dissolution, Ostwald ripening, or agglomeration, deteriorating the active centers and lowering the stability.[109] To date, there is no efficient strategy to solve these inevitable dilemmas. It should be mentioned that encapsulating the metal by a protective shell such as carbon shell may be a promising method to prolong the chemical stability of HER catalysts in AEMWE, which has been applied in other electrochemical fields.[110] For instance, Sung et al. prepared the carbon-shell-coated FeP nanoparticles via a single step heating procedure of polydopamine-coated iron oxides (Figure 4e).[111] Interestingly, the carbon-shell-coated FeP shows almost no HER activity loss after 5000 cycles, while the one without protective carbon shell has an overpotential increase of 100 mV after the same cycling tests. Detailed analysis indicates that the carbon shell provides both physical and chemical protections to prevent the aggregation of the FeP, leading to enhanced stability (Figure 4f). However, such a promising approach has not been reported to the design of stable AEMWE electrocatalysts so far, deserving further attention and exploration.

Mechanical degradation is another essential factor that limits the durability of HER electrocatalysts in AEMWE. Most of our synthesized catalysts are powdery materials, which require polymer binders such as Aemion and Fumion FAA-3 ionomers to be loaded on carriers and thus possess a weak metal−support interaction. As discussed in the last part, the high currents of AEMWE drive the violent production of a large number of gas bubbles. These insoluble bubbles will weaken the binding force and peel the catalysts off the support, undermining the operation stability of AEMWE. Similarly, an available method is to directly grow or deposit catalysts on conductive supports, which is beneficial for enhancing the metal−support interaction and mechanical stability. In addition, the porous and hydrophilic characteristics of these supported catalysts can facilitate bubble removal. Liu et al. have confirmed that the self-supported CoP on Co foam can steadily work for 4000 h at 1000 mA cm^{-2} in AEMWE (Figure 4g).[112]

In addition, different from the uninterrupted stability tests in the laboratory, the practical water electrolyzer is operated in intermittent mode for a long time, where the supply of electrolyte and the voltage will be stopped at each period of rest time. The stability of AEMWE in this mode has also been investigated by Niaz's group, who used NiFe/FeCo as the cathodic catalyst for 1000 h and found that the main reason for the deterioration in stability was due to membrane dehydration rather than catalyst deactivation. Therefore, the influence of factors other than the catalyst on the stability should also be noticed in the AEMWE.[113] It is especially worth mentioning that the U.S. Department of Energy has listed the expected target of reaching a long-term operating time of more than 50,000 h by 2040 for a practical water electrolyzer, which is much longer than the state-of-the-art catalyst at present. Therefore, more efforts should be devoted to prolonging the catalyst stability to meet the stricter requirement.

4.2.3. Cost. It is known that the cost of the electrocatalyst usually accounts for more than 60% of the total electrolyzer. Reducing the catalyst cost can effectively contribute to the promotion and commercialization of the alkaline water electrolyzer. Since only milligram-level metal precursors are needed to prepare HER electrocatalysts for half-cell tests in the laboratory, there is no obvious difference of cost in the use of noble metals or non-noble metals, and emphasis has been placed on enhancing the performances. In contrast, minimizing the amount of noble metals is extremely essential for practical application because many more catalysts are required in AEMWE. Therefore, although many noble-metal-based catalysts with excellent HER activity are reported, they are rarely considered to be employed in the practical AEMWE because of the severe cost issues. In our opinion, one available solution is to fabricate low-noble-metal or non-noble metal catalysts. Noble-metal-based single atom or cluster catalysts are representative low-noble-metal catalysts, in which the usage amount of precious metals is largely reduced and the active atom utilization efficiency is maximized. As shown in Figure 4h, we doped Pt single atoms in Ru/RuO_2 ($Pt−Ru/RuO_2$) for

https://doi.org/10.1021/jacsau.4c00898
JACS Au 2024, 4, 4639−4654

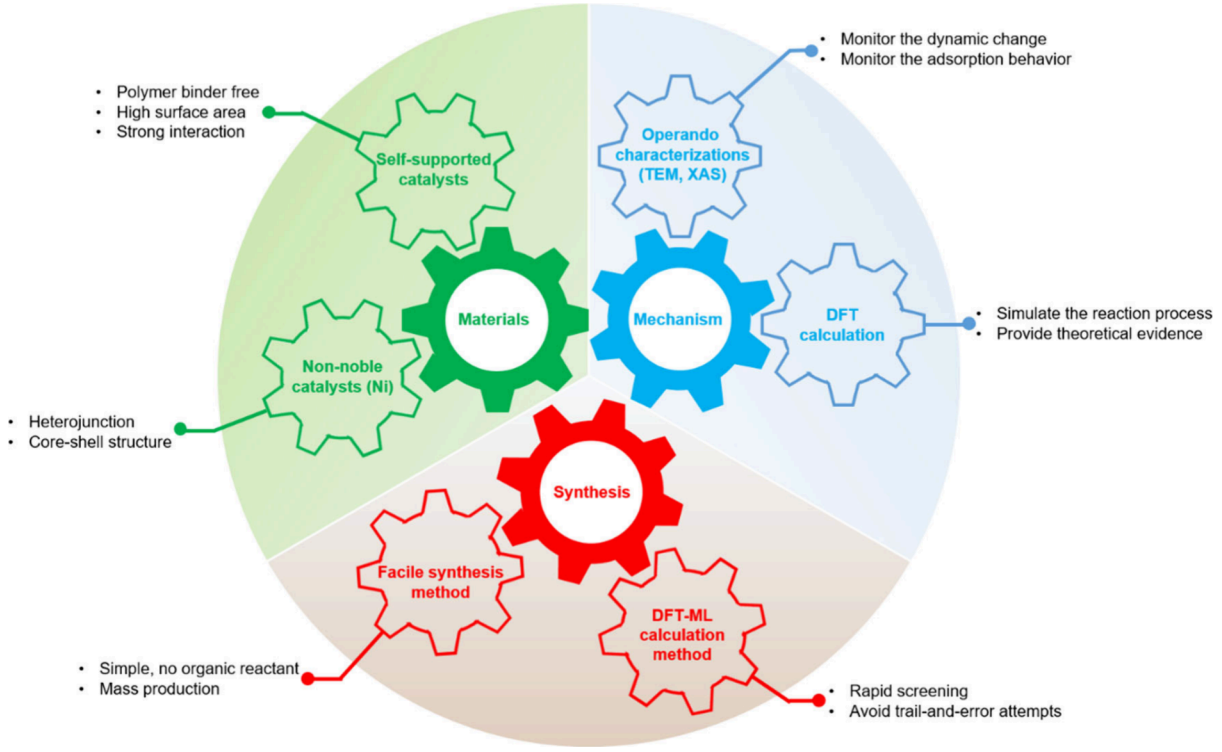

Figure 5. Outlook of the HER electrocatalysts for AEMWE: the challenges and perspectives regarding the materials, mechanism, and synthesis for the development of the HER catalysts for practical AEMWE.

alkaline HER.[97] Remarkably, in addition to excellent AEMWE performance, Pt−Ru/RuO_2 also offers superior economic advantages. After normalizing the current density to the price of the noble metal, the price activity of Pt−Ru/RuO_2 is 247.1 A dollar^{-1} at 2.1 V, which is almost 3 times higher than that of commercial Pt/C, illustrating its feasibility to be applied in practical H_2 production. Also, Guo's group designed single-atom Cr−N_4 sites with Pt atomic clusters (Pt-AC/Cr−N−C) on mesoporous carbon for alkaline HER.[114] The Pt-AC/Cr−N−C enables more stable and high-performance H_2 generation with reduced Pt usage (0.05 mg_{Pt} cm^{-2}) compared with the commercial Pt/C and other advanced Pt-based materials. In addition, as we mentioned before, accepting non-noble-metal catalysts, especially 3d transition-metal-based materials such as Ni and Co as cathodic electrocatalysts, is also a critical strategy for cost reduction. Undoubtedly, as long as the 3d transition-metal-based catalysts can be optimized to have catalytic activities exceeding those of the noble metals Pt and Ru, they are the most promising AEMWE cathode catalysts for practical industrial applications. Therefore, for the low-cost non-noble-metal catalysts, the current focus should still be placed on employing various methods to activate their activity.

Experimental procedures also possess deep influences on the cost. The cumbersome steps, including acid wash and the excessive use of reagents, would escalate the preparation and the subsequent processing costs. Moreover, the syntheses of most reported HER electrocatalysts in the laboratory are limited at the milligram-level and hard to further scale up, hence the large-scale production of electrocatalysts with negligible activity loss is imperative for practical industry to lower the cost.[91] Lots of attention has now been put on this. For example, Sung and co-workers have proved the economic efficiency caused by producing 68.281 g of the carbon-shell-coated FeP nanoparticles in one batch as the HER catalysts (Figure 4i).[111] Therefore, a facile, low-cost, and mass-production preparation method is extremely desirable for pushing the application of HER electrocatalysts forward in the AEMWE.

Besides the performance and cost, it should be noted that the H_2 production from alkaline water electrolysis is expected to be coupled with the wind, solar, and tidal energy to fully utilize the excess electricity. However, all these energy sources are intermittent energies, which poses some non-negligible challenges to the AEMWE devices, such as narrow adjustment range of the electrolyzer, slow response rate, and accelerated aging of the core components due to the frequent voltage fluctuations. Therefore, it is necessary to use the advanced power prediction technology and fast response control system to enable the AEMWE to quickly adapt to the fluctuation of these intermittent energies. In addition, a reasonable load limit should be set to ensure a gentle transition of the AEMWE during the load increase and decrease process.

5. SUMMARY AND OUTLOOK

In this perspective, we first introduce the representative descriptors for HER, which are critical for assessing and predicting the activity of electrocatalysts. We also summarize and share our thoughts on the activation strategies for exploring efficient alkaline HER electrocatalysts in light of the previously published results and our recent research achievements. Subsequently, we put emphasis on discussing the current obstacles that hinder the application of laboratory-prepared HER catalysts in the cathode of the practical AEMWE and proposing the feasible solutions to bridge these gaps, aiming at commercializing this promising technology of producing H_2 in alkaline electrolyte. In a word, the technology of AEMWE is still in its infancy, and greater endeavors are urgently yearned to design cathodic electrocatalysts with high

https://doi.org/10.1021/jacsau.4c00898
JACS Au 2024, 4, 4639−4654

performance and low cost. Some future development directions regarding to the alkaline HER electrocatalysts are proposed in Figure 5 and below.

(1) We here want to highlight the significance of fabricating self-supported electrocatalysts for sustainable large-scale generation of H_2 again.[115,116] It is known that ionomer is indispensable for powdery HER electrocatalysts to be loaded on electrode substrates, which will lead to a weak metal−support interaction (MSI), poor conductivity, and vulnerable structure of the electrocatalysts under the operating conditions of AEMWE. This is one of the prominent reasons that limit the AEMWE activity and stability of these electrocatalysts. The ionomer-free self-supported electrocatalysts with enhanced MSI can surmount the above shortcomings and meet the high demands of a practical water electrolyzer. In addition, the active sites are uniformly dispersed on the substrate surface of the self-supported electrocatalysts, which can effectively reduce the usage amount of metals and lower the preparation cost. Also, the strong adhesion between the catalysts and substrates in the self-supported electrocatalysts improves the electrical conductivity and facilitates the mass transport and kinetics. Furthermore, the loosely packed structure allows the rapid release of the generated gas bubbles on self-supported electrocatalysts, which prevents the mechanical degradation and prolongs the stability in AEMWE. Meanwhile, it should be noted that in the pure water-fed AEMWE, ionomer is an indispensable additive in the catalyst layer because of the lack of OH^- supply and transport pathway. At this time, an effective strategy is to construct an integrated electrode by uniformly spraying the anion exchange ionomer onto the self-supported electrode to simultaneously take the structural advantages of the self-supported catalysts and the anion conductivity of the ionomer, which can enhance the performance of pure water-fed AEMWE and deserve further attention. In general, all above merits endow the self-supported electrocatalysts with a promising prospect to massively produce H_2 in the practical AEMWE.

On the other hand, as we discussed before, the development of non-noble-metal catalysts with high catalytic activity holds even greater promise for the future, given the requirements of industrial applications. However, the catalytic properties of non-noble metals, especially Ni, still need to be further improved. In addition to the previously mentioned alloying, doping, and other strategies, we believe that the following points can be employed to design high-performance Ni-based HER catalysts. First, Ni-based catalysts with self-supporting structure can be designed to enhance the AEMWE stability; second, considering that alkaline HER contains a sluggish water dissociation step, it is reasonable to design the Ni-based catalysts with heterojunction or core−shell structure to introduce the efficient synergistic function or adjust the intermediate adsorption property to enhance the catalytic activity. Furthermore, we also want to highlight that the 3d transition metals have the capacity to simultaneously drive both alkaline HER and OER, which can be used as the bifunctional catalysts in the anode and cathode of AEMWE. This feature can potentially reduce the fabrication cost of the electrolyzer and simplify the overall system, thus deserving more attention.

(2) In order to provide guidance for designing high-performance electrocatalysts, figuring out how the catalytic reactions proceed is critical. Nevertheless, many short-lived intermediates are commonly generated, and reversible structural changes are possibly induced on catalysts during the reaction process, which are difficult to capture and demonstrated by ex-situ characterizations. Therefore, operando techniques are discovered, and with the assistance of these powerful tools, a deep and comprehensive understanding of the reaction mechanism is at hand. Specifically, the operando TEM (Transmission Electron Microscope) can directly provide the graphic evidence on the real-time migration and transformation of catalysts during the reaction. In addition, operando Raman and XAS (X-ray Absorption Spectroscopy) can, respectively, tell us the absorbed intermediates and the changes (structural and electronic) on catalysts under various applied reaction voltages.[117,118] While the literature on employing operando characterization technologies to investigate the reaction mechanism of HER catalysts in the three-electrode system is expanding, there are few related reports on employing these cutting-edge tools to study the dynamic changes of the catalysts in AEMWE for the time being. Due to the more demanding environments in AEMWE, an absolutely different evolution may be induced on cathodic catalysts during the reaction process, which is instructive for further promoting the performances. We also know that this is really challenging at present. For instance, the violently produced bubbles on catalysts in AEMWE scatter the laser and the X-ray, hindering the acquisition of valuable signals via operando Raman and operando XAS. We anticipate that more potent time-resolved characterization techniques can be devised in the future by optimizing the electrochemical cell, strengthening the light sources, and other measures to investigate the mechanism of HER catalysts in AEMWE and narrow the performance differences between them. In addition, the currently widely used free energy calculations are simply obtained from the energy difference of the catalyst between the elemental reaction steps, which has some limitations in disclosing the mechanism. In recent years, DFT calculations based on kinetic and thermodynamic simulation of the dynamic reaction process have gradually emerged, and we believe that this advanced and powerful calculation method will receive more attention in the future because it can simulate the energy changes of catalysts reacting in the real electrochemical environments and it can provide more persuasive theoretical evidence for the mechanism explanation.

(3) For the synthesis of basic HER catalysts applied in AEMWE, a particularly simple method needs to be developed. On the one hand, the use of polluting and expensive organic substances needs to be avoided, and on the other hand, it needs to be possible to prepare the catalysts in bulk, i.e., on a one- time basis on the scale of kilograms. This means that many of the synthesis methods currently reported in the literature, such as electrochemical deposition and impregnation, are not relevant. We believe that hydrothermal methods and ball milling may be the most promising methods for catalyst synthesis for practical industrial applications. In addition, the selection and experimental screening of most current HER catalysts still heavily rely on conducting a large number of trial-and-error reactions, which are often expensive and time-consuming. Although DFT calculations have been widely developed to provide the HER descriptors for predicting the candidates, theoretical calculations usually are on a case by case basis and use simplified models, which may result in a large deviation between the calculation results and experimental outcomes. Fortunately, accompanied by the progress of computing power and data availability, the high-

https://doi.org/10.1021/jacsau.4c00898
JACS Au 2024, 4, 4639−4654

throughput machine learning algorithms based on the integration and simulation of big data sets has further advanced the accurate and rapid screening of the high-performance HER catalysts.[119] In addition, the dynamic process and the intrinsic correlation between activity and structure can also be investigated by DFT-ML, providing atomic insights during HER.[120] In this regard, we hope that this powerful approach will play an important role in exploring more superior HER catalysts in the future, which also contributes to the development of the AEMWE.

AUTHOR INFORMATION

Corresponding Author

Jiwei Ma − *Shanghai Key Laboratory for R&D and Application of Metallic Functional Materials, Institute of New Energy for Vehicles, School of Materials Science and Engineering, Tongji University, 201804 Shanghai, China;* orcid.org/0000-0003-4209-7667; Email: jiwei.ma@tongji.edu.cn

Authors

Yiming Zhu − *Shanghai Key Laboratory for R&D and Application of Metallic Functional Materials, Institute of New Energy for Vehicles, School of Materials Science and Engineering, Tongji University, 201804 Shanghai, China*

Ling Li − *Center of Artificial Photosynthesis for Solar Fuels and Department of Chemistry, School of Science and Research Center for Industries of the Future, Westlake University, 310024 Zhejiang, China*

Hongfei Cheng − *Shanghai Key Laboratory for R&D and Application of Metallic Functional Materials, Institute of New Energy for Vehicles, School of Materials Science and Engineering, Tongji University, 201804 Shanghai, China;* orcid.org/0000-0003-4701-4795

Complete contact information is available at: https://pubs.acs.org/10.1021/jacsau.4c00898

Author Contributions

#Yiming Zhu and Ling Li contributed equally to this work. The manuscript was written through contributions of all authors. All authors have given approval to the final version of the manuscript.

Notes

The authors declare no competing financial interest.

ACKNOWLEDGMENTS

The work was supported by funding from the National Natural Science Foundation of China (22179098).

REFERENCES

(1) Hong, W. T.; Risch, M.; Stoerzinger, K. A.; Grimaud, A.; Suntivich, J.; Shao-Horn, Y. Toward the rational design of non-precious transition metal oxides for oxygen electrocatalysis. *Energy Environ. Sci.* **2015**, *8*, 1404−1427.

(2) Bockris, J. O. M. A Hydrogen Economy. *Science* **1972**, *176*, 1323.

(3) Stamenkovic, V. R.; Strmcnik, D.; Lopes, P. P.; Markovic, N. M. Energy and fuels from electrochemical interfaces. *Nat. Mater.* **2017**, *16*, 57−69.

(4) Ji, S.; Lai, C.; Zhou, H.; Wang, H.; Ma, L.; Wang, C.; Zhang, K.; Li, F.; Lei, L. In situ growth of $NiSe_2$ nanocrystalline array on graphene for efficient hydrogen evolution reaction. *Front. Energy* **2022**, *16*, 595−600.

(5) Trasatti, S. Work function, electronegativity, and electrochemical behavior of metals: III. Electrolytic hydrogen evolution in acid solutions. *J. Electroanal. Chem. Interfacial Electrochem.* **1972**, *39*, 163−184.

(6) Turner, J. A. Sustainable hydrogen production. *Science* **2004**, *305*, 972−974.

(7) Zhu, J.; Hu, L.; Zhao, P.; Lee, L. Y. S.; Wong, K.-Y. Recent advances in electrocatalytic hydrogen evolution using nanoparticles. *Chem. Rev.* **2020**, *120*, 851−918.

(8) Shi, Y.; Zhang, B. Recent advances in transition metal phosphide nanomaterials: synthesis and applications in hydrogen evolution reaction. *Chem. Soc. Rev.* **2016**, *45*, 1529−1541.

(9) Li, Y.; Pei, W.; He, J.; Liu, K.; Qi, W.; Gao, X.; Zhou, S.; Xie, H.; Yin, K.; Gao, Y.; He, J.; Zhao, J.; Hu, J.; Chan, T.-S.; Li, Z.; Zhang, G.; Liu, M. Hybrids of PtRu nanoclusters and black phosphorus nanosheets for highly efficient alkaline hydrogen evolution reaction. *ACS Catal.* **2019**, *9*, 10870−10875.

(10) Tu, K.; Tranca, D.; Rodriguez-Hernandez, F.; Jiang, K.; Huang, S.; Zheng, Q.; Chen, M. X.; Lu, C.; Su, Y.; Chen, Z.; Mao, H.; Yang, C.; Jiang, J.; Liang, H. W.; Zhuang, X. A novel heterostructure based on RuMo nanoalloys and N-doped carbon as an efficient electrocatalyst for the hydrogen evolution reaction. *Adv. Mater.* **2020**, *32*, 2005433.

(11) Jiang, J.; Liao, J.; Tao, S.; Najam, T.; Ding, W.; Wang, H.; Wei, Z. Modulation of iridium-based catalyst by a trace of transition metals for hydrogen oxidation/evolution reaction in alkaline. *Electrochim. Acta* **2020**, *333*, 135444.

(12) Zhang, J.; Zhang, L.; Liu, J.; Zhong, C.; Tu, Y.; Li, P.; Du, L.; Chen, S.; Cui, Z. OH spectator at IrMo intermetallic narrowing activity gap between alkaline and acidic hydrogen evolution reaction. *Nat. Commun.* **2022**, *13*, 5497.

(13) Liu, Z.; Jiang, J.; Liu, Y.; Huang, G.; Yuan, S.; Li, X.; Li, N. Boosted hydrogen evolution reaction based on synergistic effect of RuO_2@MoS_2 hybrid electrocatalyst. *Appl. Surf. Sci.* **2021**, *538*, 148019.

(14) Nørskov, J. K.; Christensen, C. H. Toward efficient hydrogen production at surfaces. *Science* **2006**, *312*, 1322−1323.

(15) Mahmood, J.; Li, F.; Jung, S.-M.; Okyay, M. S.; Ahmad, I.; Kim, S. J.; Park, N.; Jeong, H. Y.; Baek, J.-B. An efficient and pH-universal ruthenium-based catalyst for the hydrogen evolution reaction. *Nat. Nanotechnol.* **2017**, *12*, 441−446.

(16) Ledezma-Yanez, I.; Wallace, W. D. Z.; Sebastián-Pascual, P.; Climent, V.; Feliu, J. M.; Koper, M. T. M. Interfacial water reorganization as a pH-dependent descriptor of the hydrogen evolution rate on platinum electrodes. *Nat. Energy* **2017**, *2*, 17031−17037.

(17) Kibsgaard, J.; Tsai, C.; Chan, K.; Benck, J. D.; Nørskov, J. K.; Abild-Pedersen, F.; Jaramillo, T. F. Designing an improved transition metal phosphide catalyst for hydrogen evolution using experimental and theoretical trends. *Energy Environ. Sci.* **2015**, *8*, 3022−3029.

(18) Zheng, J.; Sheng, W.; Zhuang, Z.; Xu, B.; Yan, Y. Universal dependence of hydrogen oxidation and evolution reaction activity of platinum-group metals on pH and hydrogen binding energy. *Sci. Adv.* **2016**, *2*, e1501602−e1501609.

(19) Hao, S.; Sheng, H.; Liu, M.; Huang, J.; Zheng, G.; Zhang, F.; Liu, X.; Su, Z.; Hu, J.; Qian, Y.; Zhou, L.; He, Y.; Song, B.; Lei, L.; Zhang, X.; Jin, S. Torsion strained iridium oxide for efficient acidic water oxidation in proton exchange membrane electrolyzers. *Nat. Nanotechnol.* **2021**, *16*, 1371−1377.

(20) Carmo, M.; Fritz, D. L.; Mergel, J.; Stolten, D. A Comprehensive review on PEM water electrolysis. *Int. J. Hydrogen Energy* **2013**, *38*, 4901−4934.

(21) Yu, Q.; Zhang, Z.; Qiu, S.; Luo, Y.; Liu, Z.; Yang, F.; Liu, H.; Ge, S.; Zou, X.; Ding, B.; Ren, W.; Cheng, H. M.; Sun, C.; Liu, B. A Ta-TaS_2 monolith catalyst with robust and metallic interface for superior hydrogen evolution. *Nat. Commun.* **2021**, *12*, 6051.

(22) Yu, W.; Porosoff, M. D.; Chen, J. G. Review of Pt-based bimetallic catalysis: from model surfaces to supported catalysts. *Chem. Rev.* **2012**, *112*, 5780−5817.

(23) Cheng, N.; Stambula, S.; Wang, D.; Banis, M. N.; Liu, J.; Riese, A.; Xiao, B.; Li, R.; Sham, T. K.; Liu, L. M.; Botton, G. A.; Sun, X. Platinum single-atom and cluster catalysis of the hydrogen evolution reaction. *Nat. Commun.* **2016**, *7*, 13638.
(24) Dai, J.; Zhu, Y.; Chen, Y.; Wen, X.; Long, M.; Wu, X.; Hu, Z.; Guan, D.; Wang, X.; Zhou, C.; Lin, Q.; Sun, Y.; Weng, S.-C.; Wang, H.; Zhou, W.; Shao, Z. Hydrogen spillover in complex oxide multifunctional sites improves acidic hydrogen evolution electrocatalysis. *Nat. Commun.* **2022**, *13*, 1189.
(25) Tao, Z.; Zhao, H.; Lv, N.; Luo, X.; Yu, J.; Tan, X.; Mu, S. Crystalline/amorphous-Ru//VO_x phase engineering expedites the alkaline hydrogen evolution kinetics. *Adv. Funct. Mater.* **2024**, *34*, 2312987.
(26) Shah, A. H.; Zhang, Z.; Wan, C.; Wang, S.; Zhang, A.; Wang, L.; Alexandrova, A. N.; Huang, Y.; Duan, X. Platinum surface water orientation dictates hydrogen evolution reaction kinetics in alkaline media. *J. Am. Chem. Soc.* **2024**, *146*, 9623−9630.
(27) Xu, S.; Feng, S.; Yu, Y.; Xue, P.; Liu, M.; Wang, C.; Zhao, K.; Xu, B.; Zhang, J. Dual-site segmentally synergistic catalysis mechanism: boosting $CoFeS_x$ nanocluster for sustainable water oxidation. *Nat. Commun.* **2024**, *15*, 1720.
(28) Lei, H.; Wan, Q.; Tan, S.; Wang, Z.; Mai, W. Pt quantum dot modified S-NiFe layered double hydroxide for high-current-density alkaline water splitting at industrial temperature. *Adv. Mater.* **2023**, *35*, 2208209.
(29) Hu, Q.; Gao, K.; Wang, X.; Zheng, H.; Cao, J.; Mi, L.; Huo, Q.; Yang, H.; Liu, J.; He, C. Subnanometric Ru clusters with upshifted D band center improve performance for alkaline hydrogen evolution reaction. *Nat. Commun.* **2022**, *13*, 3958.
(30) Xu, J.; Wang, X.; Mao, X.; Feng, X.; Xu, J.; Zhong, J.; Wang, L.; Han, N.; Li, Y. Prominent electronic effect in iridium-alloy-skinned nickel nanoparticles boosts alkaline hydrogen electrocatalysis. *Energy Environ. Sci.* **2023**, *16*, 6120−6126.
(31) Cheng, X.; Li, Y.; Zheng, L.; Yan, Y.; Zhang, Y.; Chen, G.; Sun, S.; Zhang, J. Highly active, stable oxidized platinum clusters as electrocatalysts for the hydrogen evolution reaction. *Energy Environ. Sci.* **2017**, *10*, 2450−2458.
(32) Cheng, Q.; Hu, C.; Wang, G.; Zou, Z.; Yang, H.; Dai, L. Carbon-defect-driven electroless deposition of Pt atomic clusters for highly efficient hydrogen evolution. *J. Am. Chem. Soc.* **2020**, *142*, 5594−5601.
(33) Ma, H.-B.; Zhou, X.-Y.; Li, J.-Y.; Cheng, H.-F.; Ma, J.-W. Rational design of heterostructured nanomaterials for accelerating electrocatalytic hydrogen evolution reaction kinetics in alkaline media. *J. Electrochem.* **2024**, *30*, 2305101.
(34) Xu, Q.; Zhang, L.; Zhang, J.; Wang, J.; Hu, Y.; Jiang, H.; Li, C. Anion exchange membrane water electrolyzer: electrode design, lab-scaled testing system and performance evaluation. *Energychem* **2022**, *4*, 100087.
(35) Hua, D.; Huang, J.; Fabbri, E.; Rafique, M.; Song, B. Development of anion membrane water electrolysis and the associated challenges: a review. *ChemElectroChem.* **2023**, *10*, No. e202200999.
(36) Tricker, A. W.; Lee, J. K.; Shin, J. R.; Danilovic, N.; Weber, A. Z.; Peng, X. Design and operating principles for high-performing anion exchange membrane water electrolyzers. *J. Power Sources* **2023**, *567*, 232967.
(37) Shirvanian, P.; Loh, A.; Sluijter, S.; Li, X. Novel components in anion exchange membrane electrolyzers (AEMWE's): status, challenges and future needs. A mini review. *Electrochem. Commun.* **2021**, *132*, 107140.
(38) Vincent, I.; Bessarabov, D. Low cost hydrogen production by anion exchange membrane electrolysis: A review. *Renew. Sust. Energy Rev.* **2018**, *81*, 1690−1704.
(39) Du, N.; Roy, C.; Peach, R.; Turnbull, M.; Thiele, S.; Bock, C. Anion-exchange membrane water electrolyzers. *Chem. Rev.* **2022**, *122*, 11830−11895.
(40) Lee, S. A.; Kim, J.; Kwon, K. C.; Park, S. H.; Jang, H. W. Anion exchange membrane water electrolysis for sustainable large-scale hydrogen production. *Carbon Neutralization* **2022**, *1*, 26−48.
(41) Ehlers, J. C.; Feidenhans'l, A. A.; Therkildsen, K. T.; Larrazabal, G. O. Affordable green hydrogen from alkaline water electrolysis: key research needs from an industrial perspective. *ACS Energy Lett.* **2023**, *8*, 1502−1509.
(42) Xue, D.; Cheng, J.; Yuan, P.; Lu, B.-A.; Xia, H.; Yang, C.-C.; Dong, C.-L.; Zhang, H.; Shi, F.; Mu, S.-C.; Hu, J.-S.; Sun, S.-G.; Zhang, J.-N. Boron-tethering and regulative electronic states around iridium species for hydrogen evolution. *Adv. Funct. Mater.* **2022**, *32*, 2113191.
(43) Zheng, Y.; Jiao, Y.; Vasileff, A.; Qiao, S.-Z. The hydrogen evolution reaction in alkaline solution: From theory, single crystal models, to practical electrocatalysts. *Angew. Chem., Int. Ed.* **2018**, *57*, 7568−7579.
(44) Speck, F. D.; Kim, J. H.; Bae, G.; Joo, S. H.; Mayrhofer, K. J. J.; Choi, C. H.; Cherevko, S. Single-atom catalysts: A perspective toward application in electrochemical energy conversion. *JACS Au* **2021**, *1*, 1086−1100.
(45) Li, J.; Chen, C.; Xu, L.; Zhang, Y.; Wei, W.; Zhao, E.; Wu, Y.; Chen, C. Challenges and perspectives of single-atom-based catalysts for electrochemical reactions. *JACS Au* **2023**, *3*, 736−755.
(46) Liu, F.; Shi, C.; Guo, X.; He, Z.; Pan, L.; Huang, Z.-F.; Zhang, X.; Zou, J.-J. Rational design of better hydrogen evolution electrocatalysts for water splitting: A review. *Adv. Sci.* **2022**, *9*, 2200307.
(47) Gonzalez-Poggini, S. Hydrogen evolution descriptors: A review for electrocatalyst development and optimization. *Int. J. Hydrogen Energy* **2024**, *59*, 30−42.
(48) Mahmood, N.; Yao, Y.; Zhang, J.-W.; Pan, L.; Zhang, X.; Zou, J.-J. Electrocatalysts for hydrogen evolution in alkaline electrolytes: Mechanisms, challenges, and prospective solutions. *Adv. Sci.* **2018**, *5*, 1700464.
(49) Xu, H.; Cheng, D.; Cao, D.; Zeng, X. C. Revisiting the universal principle for the rational design of single-atom electrocatalysts. *Nat. Catal.* **2024**, *7*, 207−218.
(50) Rajalakshmi, R.; Srividhya, G.; Viswanathan, C.; Ponpandian, N. The intriguing bifunctional effect of strong metal support interaction (SMSI) and hydrogen spillover effect (HSPE) for effective hydrogen evolution reaction. *Appl. Catal. B: Environ.* **2023**, *339*, 123089.
(51) Li, J.; Hu, J.; Zhang, M.; Gou, W.; Zhang, S.; Chen, Z.; Qu, Y.; Ma, Y. A fundamental viewpoint on the hydrogen spillover phenomenon of electrocatalytic hydrogen evolution. *Nat. Commun.* **2021**, *12*, 3502.
(52) Laursen, A. B.; Varela, A. S.; Dionigi, F.; Fanchiu, H.; Miller, C.; Trinhammer, O. L.; Rossmeisl, J.; Dahl, S. Electrochemical hydrogen evolution: Sabatier's principle and the volcano plot. *J. Chem. Educ.* **2012**, *89*, 1595−1599.
(53) Seh, Z. W.; Kibsgaard, J.; Dickens, C. F.; Chorkendorff, I.; Nørskov, J. K.; Jaramillo, T. F. Combining theory and experiment in electrolysis: Insights into materials design. *Science* **2017**, *355*, 4998.
(54) Zheng, Y.; Jiao, Y.; Zhu, Y.; Li, L. H.; Han, Y.; Chen, Y.; Jaroniec, M.; Qiao, S.-Z. High electrocatalytic hydrogen evolution activity of an anomalous ruthenium catalyst. *J. Am. Chem. Soc.* **2016**, *138*, 16174−16181.
(55) Li, F.; Han, G.-F.; Noh, H.-J.; Jeon, J.-P.; Ahmad, I.; Chen, S.; Yang, C.; Bu, Y.; Fu, Z.; Lu, Y.; Baek, J.-B. Balancing hydrogen adsorption/desorption by orbital modulation for efficient hydrogen evolution catalysis. *Nat. Commun.* **2019**, *10*, 4060.
(56) Song, F.; Li, W.; Yang, J.; Han, G.; Liao, P.; Sun, Y. Interfacing nickel nitride and nickel boosts both electrocatalytic hydrogen evolution and oxidation reactions. *Nat. Commun.* **2018**, *9*, 4531.
(57) Mao, B.; Sun, P.; Jiang, Y.; Meng, T.; Guo, D.; Qin, J.; Cao, M. Identifying the transfer kinetics of adsorbed hydroxyl as a descriptor of alkaline hydrogen evolution reaction. *Angew. Chem.* **2020**, *132*, 15344−15349.

https://doi.org/10.1021/jacsau.4c00898
JACS Au 2024, 4, 4639−4654

(58) Shen, L.-F.; Lu, B.-A.; Li, Y.-Y.; Liu, J.; Huang-fu, Z.-C.; Peng, H.; Ye, J.-Y.; Qu, X.-M.; Zhang, J.-M.; Li, G.; Cai, W.-B.; Jiang, Y.-X.; Sun, S.-G. Interfacial structure of water as a new descriptor of the hydrogen evolution reaction. *Angew. Chem. Inter. Ed.* **2020**, *59*, 22397−22402.
(59) Zhao, Z.-J.; Liu, S.; Zha, S.; Cheng, D.; Studt, F.; Henkelman, G.; Gong, J. Theory-guided design of catalytic materials using scaling relationships and reactivity descriptors. *Nat. Rev. Mater.* **2019**, *4*, 792−804.
(60) Sun, S.; Zhou, X.; Cong, B.; Hong, W.; Chen, G. Tailoring the d-band centers endows $(Ni_xFe_{1-x})_2P$ nanosheets with efficient oxygen evolution catalysis. *ACS Catal.* **2020**, *10*, 9086−9097.
(61) Zhu, Q.; Huang, W.; Huang, C.; Gao, L.; Su, Y.; Qiao, L. The *d* band center as an indicator for the hydrogen solution and diffusion behaviors in transition metals. *Int. J. Hydrogen Energy* **2022**, *47*, 38445−38454.
(62) Toyoda, E.; Jinnouchi, R.; Hatanaka, T.; Morimoto, Y.; Mitsuhara, K.; Visikovskiy, A.; Kido, Y. The d-band structure of Pt nanoclusters correlated with the catalytic activity for an oxygen reduction reaction. *J. Phys. Chem. C* **2011**, *115*, 21236−21240.
(63) Wei, C.; Sun, Y.; Scherer, G. G.; Fisher, A. C.; Sherburne, M.; Ager, J. W.; Xu, Z. J. Surface composition dependent ligand effect in tuning the activity of nickel-copper bimetallic electrocatalysts toward hydrogen evolution in alkaline. *J. Am. Chem. Soc.* **2020**, *142*, 7765−7775.
(64) Liu, C.; Sheng, B.; Zhou, Q.; Xia, Y.; Zou, Y.; Chimtali, P. J.; Cao, D.; Chu, Y.; Zhao, S.; Long, R.; Chen, S.; Song, L. Manipulating d-band center of nickel by single-iodine-atom strategy for boosted alkaline hydrogen evolution reaction. *J. Am. Chem. Soc.* **2024**, *146*, 26844−26854.
(65) Qian, S.; Xu, F.; Fan, Y.; Cheng, N.; Xue, H.; Yuan, Y.; Gautier, R.; Jiang, T.; Tian, J. Tailoring coordination environments of single-atom electrocatalysts for hydrogen evolution by topological heteroatom transfer. *Nat. Commun.* **2024**, *15*, 2774.
(66) Liu, M.; Zhang, J.; Su, H.; Jiang, Y.; Zhou, W.; Yang, C.; Bo, S.; Pan, J.; Liu, Q. In situ modulating coordination fields of single-atom cobalt catalyst for enhanced oxygen reduction reaction. *Nat. Commun.* **2024**, *15*, 1675.
(67) Shi, M.-M.; Bao, D.; Yan, J.-M.; Zhong, H.-X.; Zhang, X.-B. Coordination and architecture regulation of electrocatalysts for sustainable hydrogen energy conversion. *Acc. Mater. Res.* **2024**, *5*, 160−172.
(68) Liu, T.; Zhang, W.; Chen, T.; Liu, D.; Cao, L.; Ding, T.; Liu, X.; Pang, B.; Wang, S.; Wang, L.; Luo, Q.; Yao, T. Regulating the coordination environment of ruthenium clusters catalysts for the alkaline hydrogen evolution reaction. *J. Phys. Chem. Lett.* **2021**, *12*, 8016−8023.
(69) Pohl, M. D.; Watzele, S.; Calle-Vallejo, F.; Bandarenka, A. S. Nature of highly active electrocatalytic sites for the hydrogen evolution reaction at Pt electrodes in acidic media. *ACS Omega* **2017**, *2*, 8141−8147.
(70) Razmjooei, F.; Singh, K. P.; Yang, D.-S.; Cui, W.; Jang, Y. H.; Yu, J.-S. Fe-treated heteroatom (S/N/B/P)-doped graphene electrocatalysts for water oxidation. *ACS Catal.* **2017**, *7*, 2381−2391.
(71) Ran, N.; Qiu, W.; Song, E.; Wang, Y.; Zhao, X.; Liu, Z.; Liu, J. Bond electronegativity as hydrogen evolution reaction catalyst descriptor for transition metal (TM = Mo, W) dichalcogenides. *Chem. Mater.* **2020**, *32*, 1224−1234.
(72) Guan, D.; Zhou, J.; Huang, Y.-C.; Dong, C.-L.; Wang, J.-Q.; Zhou, W.; Shao, Z. Screening highly active perovskites for hydrogen-evolving reaction via unifying ionic electronegativity descriptor. *Nat. Commun.* **2019**, *10*, 3755.
(73) Zhang, X.-L.; Yu, P.-C.; Su, X.-Z.; Hu, S.-J.; Shi, L.; Wang, Y.-H.; Yang, P.-P.; Gao, F.-Y.; Wu, Z.-Z.; Chi, L.-P.; Zheng, Y.-R.; Gao, M.-R. Efficient acidic hydrogen evolution in proton exchange membrane electrolyzers over a sulfur-doped marcasite-type electrocatalyst. *Sci. Adv.* **2023**, *9*, No. eadh2885.
(74) Guan, D.; Xu, H.; Zhang, Q.; Huang, Y.-C.; Shi, C.; Chang, Y.-C.; Xu, X.; Tang, J.; Gu, Y.; Pao, C.-W.; Haw, S.-C.; Chen, J.-M.; Hu, Z.; Ni, M.; Shao, Z. Identifying a universal activity descriptor and a unifying mechanism concept on perovskite oxides for green hydrogen production. *Adv. Mater.* **2023**, *35*, 2305074.
(75) Dubouis, N.; Grimaud, A. The hydrogen evolution reaction: from material to interfacial descriptors. *Chem. Sci.* **2019**, *10*, 9165−9181.
(76) Wang, R.; Chen, Q.; Liu, X.; Hu, Y.; Cao, L.; Dong, B. Synergistic effects of dual-doping with Ni and Ru in monolayer VS_2 nanosheet: unleashing enhanced performance for acidic HER through defects and strain. *Small* **2024**, *20*, 2311217.
(77) Li, C.; Jang, H.; Liu, S.; Kim, M. G.; Hou, L.; Liu, X.; Cho, J. P and Mo dual doped Ru ultrasmall nanoclusters embedded in P-doped porous carbon toward efficient hydrogen evolution reaction. *Adv. Energy Mater.* **2022**, *12*, 2200029.
(78) Sun, T.; Wang, J.; Chi, X.; Lin, Y.; Chen, Z.; Ling, X.; Qiu, C.; Xu, Y.; Song, L.; Chen, W.; Su, C. Engineering the electronic structure of MoS_2 nanorods by N and Mn dopants for ultra-efficient hydrogen production. *ACS Catal.* **2018**, *8*, 7585−7592.
(79) Chi, J.-Q.; Zeng, X.-J.; Shang, X.; Dong, B.; Chai, Y.-M.; Liu, C.-G.; Marin, M.; Yin, Y. Embedding RhP_x in N, P co-doped carbon nanoshells through synergistic phosphorization and pyrolysis for efficient hydrogen evolution. *Adv. Funct. Mater.* **2019**, *29*, 1901790.
(80) Liu, C.; Pan, G.; Liang, N.; Hong, S.; Ma, J.; Liu, Y. Ir single atom catalyst loaded on amorphous carbon materials with high HER activity. *Adv. Sci.* **2022**, *9*, 2105392.
(81) Wang, L.; Ma, M.; Zhang, C.; Chang, H.-H.; Zhang, Y.; Li, L.; Chen, H.-Y.; Peng, S. Manipulating the microenvironment of single atoms by switching support crystallinity for industrial hydrogen evolution. *Angew. Chem., Int. Ed.* **2024**, *63*, No. e202317220.
(82) Cheng, X.; Mao, C.; Tian, J.; Xia, M.; Yang, L.; Wang, X.; Wu, Q.; Hu, Z. Correlation between heteroatom coordination and hydrogen evolution for single-site Pt on carbon-based nanocages. *Angew. Chem., Int. Ed.* **2024**, *63*, No. e202401304.
(83) Zhang, C.; Dai, L. Targeted defect synthesis for improved electrocatalytic performance. *Chem.* **2020**, *6*, 1847−1860.
(84) Zhang, H.; Li, K.; Guo, X.; Zhang, L.; Cao, D.; Cheng, D. Rational regulation of the defect density in platinum nanocrystals for highly efficient hydrogen evolution reaction. *Small* **2024**, *20*, 2306694.
(85) Qin, Q.; Jang, H.; Jiang, X.; Wang, L.; Wang, X.; Kim, M. G.; Liu, S.; Liu, X.; Cho, J. Constructing interfacial oxygen vacancy and ruthenium Lewis acid-base pairs to boost the alkaline hydrogen evolution reaction kinetics. *Angew. Chem., Int. Ed.* **2024**, *63*, No. e202317622.
(86) Ma, H.; Yan, W.; Yu, Y.; Deng, L.; Hong, Z.; Song, L.; Li, L. Phosphorus vacancies improve the hydrogen evolution of MoP electrocatalysts. *Nanoscale* **2023**, *15*, 1357−1364.
(87) Liu, B.; Wang, Y.; Peng, H.-Q.; Yang, R.; Jiang, Z.; Zhou, X.; Lee, C.-S.; Zhao, H.; Zhang, W. Iron vacancies induced bifunctionality in ultrathin feroxyhyte nanosheets for overall water splitting. *Adv. Mater.* **2018**, *30*, 1803144.
(88) Xie, J.; Li, S.; Zhang, X.; Zhang, J.; Wang, R.; Zhang, H.; Pan, B.; Xie, Y. Atomically-thin molybdenum nitride nanosheets with exposed active surface sites for efficient hydrogen evolution. *Chem. Sci.* **2014**, *5*, 4615−4620.
(89) Long, X.; Li, G.; Wang, Z.; Zhu, H.; Zhang, T.; Xiao, S.; Guo, W.; Yang, S. Metallic iron-nickel sulfide ultrathin nanosheets as a highly active electrocatalyst for hydrogen evolution reaction in acidic media. *J. Am. Chem. Soc.* **2015**, *137*, 11900−11903.
(90) Zhu, Y.; Zhu, X.; Bu, L.; Shao, Q.; Li, Y.; Hu, Z.; Chen, C.-T.; Pao, C.-W.; Yang, S.; Huang, X. Single-atom In-doped subnanometer Pt nanowires for simultaneous hydrogen generation and biomass upgrading. *Adv. Funct. Mater.* **2020**, *30*, 2004310.
(91) Shang, X.; Rao, Y.; Lu, S.-S.; Dong, B.; Zhang, L.-M.; Liu, X.-H.; Li, X.; Liu, Y.-R.; Chai, Y.-M.; Liu, C.-G. Novel WS_2/WO_3 heterostructured nanosheets as efficient electrocatalyst for hydrogen evolution reaction. *Mater. Chem. Phys.* **2017**, *197*, 123−128.
(92) Zhu, Y.; Peng, J.; Zhu, X.; Bu, L.; Shao, Q.; Pao, C.-W.; Hu, Z.; Li, Y.; Wu, J.; Huang, X. A large-scalable, surfactant-free, and

https://doi.org/10.1021/jacsau.4c00898
JACS Au 2024, 4, 4639−4654

ultrastable Ru-doped Pt_3Co oxygen reduction catalyst. *Nano Lett.* **2021**, *21*, 6625−6632.
(93) Wang, J.; Yan, M.; Zhao, K.; Liao, X.; Wang, P.; Pan, X.; Yang, W.; Mai, L. Field effect enhanced hydrogen evolution reaction of MoS_2 nanosheets. *Adv. Mater.* **2017**, *29*, 1604464.
(94) Xu, X.; Liu, X.; Zhong, W.; Liu, G.; Zhang, L.; Du, Y. Magnetic field improvement of hydrogen evolution reaction in MOF-derived $NiCo_2S_4$ nanostructure. *Ceram. Int.* **2023**, *49*, 16836−16841.
(95) Chen, L.; Wang, H.-Y.; Tian, W.-W.; Wang, L.; Sun, M.-L.; Ren, J.-T.; Yuan, Z.-Y. Enabling internal electric field in heterogeneous nanosheets to significantly accelerate alkaline hydrogen electrocatalysis. *Small* **2024**, *20*, 2307252.
(96) Song, B.; Jin, S. Two are better than one: Heterostructures improve hydrogen evolution catalysis. *Joule* **2017**, *1*, 220−228.
(97) Zhu, Y.; Klingenhof, M.; Gao, C.; Koketsu, T.; Weiser, G.; Pi, Y.; Liu, S.; Sui, L.; Hou, J.; Li, J.; Jiang, H.; Xu, L.; Huang, W.-H.; Pao, C.-W.; Yang, M.; Hu, Z.; Strasser, P.; Ma, J. Facilitating alkaline hydrogen evolution reaction on the hetero-interfaced Ru/RuO_2 through Pt single atoms doping. *Nat. Commun.* **2024**, *15*, 1447.
(98) Dao, V.; Di Liberto, G.; Yadav, S.; Uthirakumar, P.; Chen, K.; Pacchioni, G.; Lee, I.-H. Pt single atoms supported on defect ceria as an active and stable dual-site catalyst for alkaline hydrogen evolution. *Nano Lett.* **2024**, *24*, 1261−1267.
(99) Wang, X.; Long, G.; Liu, B.; Li, Z.; Gao, W.; Zhang, P.; Zhang, H.; Zhou, X.; Duan, R.; Hu, W.; Li, C. Rationally modulating the functions of Ni_3Sn_2-$NiSnO_x$ nanocomposites electrocatalysts towards enhanced hydrogen evolution reaction. *Angew. Chem., Int. Ed.* **2023**, *62*, No. e202301562.
(100) Zhou, K. L.; Wang, Z.; Han, C. B.; Ke, X.; Wang, C.; Jin, Y.; Zhang, Q.; Liu, J.; Wang, H.; Yan, H. Platinum single-atom catalyst coupled with transition metal/metal oxide heterostructure for accelerating alkaline hydrogen evolution reaction. *Nat. Commun.* **2021**, *12*, 3783.
(101) Wei, J.; Xiao, K.; Chen, Y.; Guo, X.-P.; Huang, B.; Liu, Z.-Q. In situ precise anchoring of Pt single atoms in spinel Mn_3O_4 for a highly efficient hydrogen evolution reaction. *Energy Environ. Sci.* **2022**, *15*, 4592−4600.
(102) Zhu, Y.; Wang, J.; Ma, J. Recent progress on non-carbon-supported single-atom catalysts for electrochemical conversion of green energy. *Small Sci.* **2023**, *3*, 2300010.
(103) Fang, Z.; Ye, C.; Ling, T.; Ji, H.; Lu, C.; Ke, C.; Zhuang, X.; Shan, J. Stability challenges of anion-exchange membrane water electrolyzers from components to integration level. *Chem. Catal.* **2024**, *4*, 101145.
(104) Galkina, I.; Faid, A. Y.; Jiang, W.; Scheepers, F.; Borowski, P.; Sunde, S.; Shviro, M.; Lehnert, W.; Mechler, A. K. Stability of Ni-Fe-layered double hydroxide under long-term operation in AEM water electrolysis. *Small* **2024**, *20*, 2311047.
(105) Zhong, X.; Sui, L.; Yang, M.; Koketsu, T.; Klingenhof, M.; Selve, S.; Reeves, K. G.; Ge, C.; Zhuang, L.; Kan, W. H.; Avdeev, M.; Shu, M.; Alonso-Vante, N.; Chen, J.-M.; Haw, S.-C.; Pao, C.-W.; Chang, Y.-C.; Huang, Y.; Hu, Z.; Strasser, P.; Ma, J. Stabilization of layered lithium-rich manganese oxide for anion exchange membrane fuel cells and water electrolysers. *Nat. Catal.* **2024**, *7*, 546−559.
(106) Lin, X.; Hu, W.; Xu, J.; Liu, X.; Jiang, W.; Ma, X.; He, D.; Wang, Z.; Li, W.; Yang, L.-M.; Zhou, H.; Wu, Y. Alleviating OH blockage on the catalyst surface by the puncture effect of single-atom sites to boost alkaline water electrolysis. *J. Am. Chem. Soc.* **2024**, *146*, 4883−4891.
(107) Yao, R.; Sun, K.; Zhang, K.; Wu, Y.; Du, Y.; Zhao, Q.; Liu, G.; Chen, C.; Sun, Y.; Li, J. Stable hydrogen evolution reaction at high current densities via designing the Ni single atoms and Ru nanoparticles linked by carbon bridges. *Nat. Commun.* **2024**, *15*, 2218.
(108) Park, Y. S.; Lee, J. H.; Jang, M. J.; Jeong, J.; Park, S. M.; Choi, W.-S.; Kim, Y.; Yang, J.; Choi, S. M. Co_3S_4 nanosheets on Ni foam via electrodeposition with sulfurization as highly active electrocatalysts for anion exchange membrane electrolyzer. *Int. J. Hydrogen Energy* **2020**, *45*, 36−45.
(109) Wan, Y.; Zhou, L.; Lv, R. Rational design of efficient electrocatalysts for hydrogen production by water electrolysis at high current density. *Mater. Chem. Front.* **2023**, *7*, 6035−6060.
(110) Yoo, J. M.; Shin, H.; Chung, D. Y.; Sung, Y.-E. Carbon shell on active nanocatalyst for stable electrocatalysis. *Acc. Chem. Res.* **2022**, *55*, 1278−1289.
(111) Chung, D. Y.; Jun, S. W.; Yoon, G.; Kim, H.; Yoo, J. M.; Lee, K.-S.; Kim, T.; Shin, H.; Sinha, A. K.; Kwon, S. G.; Kang, K.; Hyeon, T.; Sung, Y.-E. Large-scale synthesis of carbon-shell-coated FeP nanoparticles for robust hydrogen evolution reaction electrocatalyst. *J. Am. Chem. Soc.* **2017**, *139*, 6669−6674.
(112) Li, Y.; Wei, B.; Yu, Z.; Bondarchuk, O.; Araujo, A.; Amorim, I.; Zhang, N.; Xu, J.; Neves, I. C.; Liu, L. Bifunctional porous cobalt phosphide foam for high-current-density alkaline water electrolysis with 4000-h long stability. *ACS Sustainable Chem. Eng.* **2020**, *8*, 10193−10200.
(113) Niaz, A. K.; Akhtar, A.; Park, J.-Y.; Lim, H.-T. Effects of the operation mode on the degradation behavior of anion exchange membrane water electrolyzers. *J. Power Sources* **2021**, *481*, 229093.
(114) Zeng, L.; Zhao, Z.; Huang, Q.; Zhou, C.; Chen, W.; Wang, K.; Li, M.; Lin, F.; Luo, H.; Gu, Y.; Li, L.; Zhang, S.; Lv, F.; Lu, G.; Luo, M.; Guo, S. Single-atom Cr-N_4 sites with high oxophilicity interfaced with Pt atomic clusters for practical alkaline hydrogen evolution catalysis. *J. Am. Chem. Soc.* **2023**, *145*, 21432−21441.
(115) Yang, H.; Driess, M.; Menezes, P. W. Self-supported electrocatalysts for practical water electrolysis. *Adv. Energy Mater.* **2021**, *11*, 2102074.
(116) Sun, H.; Yan, Z.; Liu, F.; Xu, W.; Cheng, F.; Chen, J. Self-supported transition-metal-based electrocatalysts for hydrogen and oxygen evolution. *Adv. Mater.* **2020**, *32*, 1806326.
(117) Li, X.; Yang, X.; Zhang, J.; Huang, Y.; Liu, B. In situ/operando techniques for characterization of single-atom catalysts. *ACS Catal.* **2019**, *9*, 2521−2531.
(118) Li, J.; Gong, J. Operando characterization techniques for electrocatalysis. *Energy Environ. Sci.* **2020**, *13*, 3748−3779.
(119) Sun, M.; Dougherty, A. W.; Huang, B.; Li, Y.; Yan, C.-H. Accelerating atomic catalyst discovery by theoretical calculations-mechine-learning strategy. *Adv. Energy Mater.* **2020**, *10*, 1903949.
(120) Badreldin, A.; Bouhali, O.; Abdel-Wahab, A. Complimentary computational cues for water electrocatalysis: A DFT and ML perspective. *Adv. Funct. Mater.* **2024**, *34*, 2312425.

https://doi.org/10.1021/jacsau.4c00898
JACS Au 2024, 4, 4639−4654